



Universiteit  
Leiden  
The Netherlands

## **Towards a tailored therapeutic approach for vulvar cancer patients**

Kortekaas, K.E.

### **Citation**

Kortekaas, K. E. (2021, May 27). *Towards a tailored therapeutic approach for vulvar cancer patients*. Retrieved from <https://hdl.handle.net/1887/3180650>

Version: Publisher's Version

License: [Licence agreement concerning inclusion of doctoral thesis in the Institutional Repository of the University of Leiden](#)

Downloaded from: <https://hdl.handle.net/1887/3180650>

**Note:** To cite this publication please use the final published version (if applicable).

Cover Page



Universiteit Leiden



The handle <https://hdl.handle.net/1887/3180650> holds various files of this Leiden University dissertation.

**Author:** Kortekaas, K.E.

**Title:** Towards a tailored therapeutic approach for vulvar cancer patients

**Issue Date:** 2021-05-27

# 6

HIGH NUMBERS OF ACTIVATED HELPER T CELLS  
ARE ASSOCIATED WITH BETTER CLINICAL  
OUTCOME IN EARLY STAGE VULVAR CANCER,  
IRRESPECTIVE OF HPV OR P53 STATUS

K.E. Kortekaas, S.J.A.M. Santegoets, Z. Abdulrahman, J.J. van Ham, M.  
van der Tol, I. Ehsan, H.C. van Doorn, T. Bosse,  
M.I.E. van Poelgeest\*, S.H. van der Burg\*

\*These authors contributed equally to this work

*Journal of Immunotherapy of Cancer 2019*

## ABSTRACT

### Objective

Vulvar squamous cell carcinoma (VSCC) has been suggested to consist of three subtypes; HPV-associated, HPV-independent mutated *TP53* or HPV-independent *TP53* wildtype, with different clinical courses. To analyze the immune infiltrate in these molecular subtypes and its impact on clinical outcome, an in-depth study of the tumor immune microenvironment was performed.

### Methods

Sixty-five patients with invasive VSCC matched for age, FIGO stage and treatment modality, were grouped according to the presence of HPV and p53 protein expression pattern. Archived tissues were analyzed for intraepithelial and stromal expression of CD3, CD8, Foxp3, PD-1, and pan-keratin in randomly selected areas using immunofluorescence. Additional phenotyping of T cells was performed *ex-vivo* on VSCC ( $n=14$ ) and blood samples by flow cytometry. Healthy vulvar samples and blood served as controls.

### Results

Based on T cell infiltration patterns about half of the VSCC were classified as inflamed or altered-excluded while one-third was deserted. High intraepithelial helper T cell infiltration was observed in 78% of the HPV-associated VSCC, 60% of the HPVneg/p53wildtype VSCC and 40% of the HPVneg/p53 mutant VSCC. A high intraepithelial infiltration with activated ( $CD3^+PD-1^+$ ), specifically helper T cells ( $CD3^+CD8^-Foxp3^-$ ), was associated with a longer recurrence-free period and overall survival, irrespective of HPV and p53 status. Flow cytometry confirmed the tumor-specific presence of activated ( $CD4^+PD-1^{++}CD161^-CD38^+HLA-DR^+$  and  $CD8^+CD103^+CD161^-NKG2A^{+/-}PD-1^{++}CD38^{++}HLA-DR^+$ ) effector memory T cells.

### Conclusions

This is the first study demonstrating an association between intraepithelial T cells and clinical outcome in VSCC. Our data suggest that p53 mutant VSCCs mostly are cold tumors whereas HPV-associated VSCCs are strongly T cell infiltrated.

## INTRODUCTION

Immunotherapy of cancer has established itself as a new breakthrough approach that offers long-term durable clinical responses in patients with advanced cancers. As the initiation and regulation of the immune response to tumors is complex and multistep in nature, inspection of the different processes involved is required to provide the optimal (combination) of immunotherapeutic modalities available.<sup>1</sup> This is highly relevant for vulvar squamous cell carcinoma (VSCC), the predominant histologic subtype of vulvar cancers, for which new treatment options are urgently needed. Because despite current treatment, consisting of radical surgery and/or (chemo)radiotherapy which causes impressive morbidity, lymphedema, sexual and psychological dysfunction and wound healing disorders<sup>2,3</sup>, 46% of VSCC patients still develop recurrences after 10-years.<sup>4</sup>

At this point, however, little is known about the role and impact of cellular immunity on the clinical outcome of VSCC. Both CD4 and CD8 T cells as well as B cells infiltrate VSCC.<sup>5-7</sup> The CD4 cells comprise CD4<sup>+</sup> helper T cells and regulatory T cells (Tregs). Often a strong infiltration with one type of T cells is paralleled by the others.<sup>5,6,8</sup> In three studies focusing on the prognostic role of CD4<sup>+</sup> and/or CD8<sup>+</sup> T cells or Tregs no impact on clinical outcome was found.<sup>6,9,10</sup> On the one hand, these analyses may have been influenced by the heterogeneity of the study group with respect to tumor etiology, stage, and treatment. Furthermore, enumeration of all T cells, irrespective of their location in the tumor<sup>9</sup>, as well as preselection of highly infiltrated areas only<sup>6,10</sup>, may also have influenced study outcomes. On the other hand, the impact of T cells may be nullified by the presence of immune regulatory mechanisms, as VSCC can be massively infiltrated with M2 macrophages and Tregs.<sup>8</sup> Moreover, VSCC can express the immunoregulatory enzyme, indoleamine 2,3-dioxygenase (IDO) or PD-L1, both of which were shown to negatively influence clinical outcome.<sup>10,11</sup> Notably, PD-L1 was mainly expressed in lymphocyte rich areas<sup>11</sup>, suggesting that it functioned as an adaptive escape mechanism<sup>12</sup>, and implying that in some VSCC a functionally active antitumor response is present. This notion is sustained by the observation that the intraepithelial presence of Granzyme B-positive cells is related to better overall survival (OS) in patients with localized VSCC.<sup>13</sup>

At present, three distinct etiologic pathways in the development of VSCC have been proposed. One type is driven by the overexpression of high-risk human papilloma virus oncogenes E6 and E7 (HPVpos VSCC). The second type is not related to HPV and can be categorized based on the mutational status of the tumor suppressor gene *TP53* associated with high protein levels of p53 (HPVneg/p53mut VSCC). We recently identified a third type as a substantial group of patients with a HPV-independent VSCC displaying normal expression levels of p53 protein (HPVneg/p53wt VSCC) but frequently bearing other mutations.<sup>14</sup> Importantly, HPV-associated VSCC display better OS and a longer recurrence-free period (RFP) than HPVneg

VSCC.<sup>14-17</sup> Interestingly among the latter group, local recurrences more often occurred after treatment in patients with HPVneg/p53mut VSCC than in HPVneg/p53wt VSCC.<sup>14</sup> With the first reports showing an influence of different oncogenic pathways on local immunity<sup>18,19</sup>, we asked the question if the differences in RFP and OS observed between these three different groups of VSCC could be explained by the local immune response. Bearing in mind the limitations of previous studies, we selected three cohorts of VSCCs based on their HPV and p53 protein (wt/mut) status which were highly matched for clinicopathological parameters and enumerated different types of intraepithelial and stromal T cells in randomly selected fields of VSCC, using multiplex immunofluorescence. In-depth analysis of T cells was performed on freshly dispersed tissue by flow cytometry.

Our study revealed a strong impact of intraepithelial activated T cells on clinical outcome, in particular a dense infiltration with intraepithelial CD4<sup>+</sup> T cells was highly associated with RFP and OS, irrespective of HPV or p53 status. Moreover, the percentage of tumors highly infiltrated with these T cells varied between the three different subtypes, with HPV-associated VSCC most often strongly infiltrated (78%) followed by the HPVneg/p53wt VSCC (60%) and the lowest infiltration in the HPVneg/p53mut VSCC group (40%).

## **MATERIAL AND METHODS**

### **Patient materials**

Archived formalin-fixed paraffin-embedded (FFPE) tumor tissue from VSCC patients was selected from a larger cohort with known HPV and p53 status. HPV presence was tested by HPV-PCR and p16 IHC.<sup>20</sup> Tumors that were positive in both tests were assigned as HPVpos VSCC. When both tests were negative, tumors were scored as HPVneg VSCC. The HPVneg VSCC were further sub-classified based on the wildtype or mutant expression of p53 (HPVneg/p53wt VSCC and HPVneg/p53mut VSCC) as previously described.<sup>14</sup> In addition, archived FFPE healthy HPV-independent vulvar tissue from 10 women who underwent labial reduction surgery served as controls. Fresh tumor tissue ( $n=14$ ) and blood samples ( $n=34$ ) were obtained from 38 patients participating in the large observational CIRCLE study. Women with histologically proven p16<sup>ink4a</sup>-negative VSCC were included in this study investigating cellular immunity against anogenital lesions.<sup>21, 22</sup> Tumor staging was done according to FIGO staging 2009. Patients were included after signing informed consent. The study was conducted in accordance with the Declaration of Helsinki and approved by the local medical ethical committee of the Leiden University Medical Center (P08.197 and B16.024) and in agreement with the Dutch law. The materials were used according to the Dutch Federation of Medical Research Association guidelines. The patients received standard-of-care treatment consisting of primary surgery.

### **Multiplex six color staining, image acquisition and analysis by VECTRA**

For the direct and indirect immunofluorescent six color staining and detection, 4 $\mu$ m FFPE tissue sections were deparaffinized and prepared with heat-induced antigen citrate (10mM, pH 6.0) retrieval as described previously.<sup>23</sup> Antibody specificity and optimal conditions for antigen retrieval were assessed by single-plex immunohistochemistry (IHC) using tonsils as a positive control.<sup>23</sup> After incubation with superblock buffer (Thermo Fisher Scientific, Waltham, MA, USA), the primary antibodies and isotype/species-specific secondary fluorescent antibodies were applied (supplemental table 1). Nuclear counterstain was obtained with DAPI. Tissue slides were imaged at 20x magnification with the Vectra 3.0 Automated Quantitative Pathology Imaging System (Perkin Elmer). Imaging analysis and spectral separation of dyes was performed with the InForm Cell Analysis software (Perkin Elmer) by using spectral libraries defined with single-marker immunofluorescence detection. Five random multispectral imaging fields of interest were selected for acquisition from each tumor, depending on its size. Tissue and cellular segmentation was done as described before.<sup>23</sup> The following phenotypes were identified for the T cell panel: total T cells (CD3<sup>+</sup>), CD8<sup>+</sup> T cells (CD3<sup>+</sup>CD8<sup>+</sup>Foxp3<sup>-</sup>), helper T cells (CD3<sup>+</sup>CD8<sup>-</sup>Foxp3<sup>+</sup>), Tregs (CD3<sup>+</sup>CD8<sup>-</sup>Foxp3<sup>+</sup>), PD-1 expressing T cells (CD3<sup>+</sup>PD-1<sup>+</sup>). All images were visually inspected to confirm the correct attribution and quantification of phenotypes, and segmentation of tissue. Because PD-1 could be expressed by CD3<sup>+</sup>CD8<sup>-</sup> and CD3<sup>+</sup>CD8<sup>+</sup> cells, the CD3<sup>+</sup>PD-1<sup>+</sup> phenotypes were separately analyzed. All phenotypes in both areas were normalized by tissue area (number of cells/mm<sup>2</sup>). In addition, ten HPVpos VSCC, six HPVneg/53wt VSCC and five HPVneg/p53mut VSCC samples were used to study Tbet (Santa Cruz, clone H-210, dilution 1:100) expressing CD3<sup>+</sup> cells with immunofluorescence.

### **Blood and tumor cell isolation and culturing**

Venous blood samples were drawn prior to surgery, and peripheral blood mononuclear cells (PBMC) were isolated using Ficoll density gradient centrifugation as described previously.<sup>24, 25</sup> VSCC tumor material was obtained and handled as described.<sup>24, 25</sup> First, tumor material was cut into small pieces. One-third of the tumor pieces was incubated for 60 minutes at 37°C in Iscove's Modified Dulbecco's Medium (IMDM, Gibco by life technologies, ThermoFisher Scientific, Lonza, Verviers, Belgium) with 10% human AB serum (Capricorn Scientific, Esdorfergrund, Germany) and supplemented with high dose of antibiotics (50  $\mu$ g/ml Gentamycin (Gibco/ Thermo Fisher Scientific (TFS), Bleiswijk, the Netherlands), 25  $\mu$ g/ml Fungizone (Gibco/Thermo Fisher Scientific), after which the tumor pieces were put in culture in IMDM supplemented with 10% human AB serum (IMDM complete) and 1000 IU/ml human recombinant IL-2 (Aldesleukin, Novartis, Arnhem, the Netherlands). Cultures ( $n=14$ ) were replenished every 2-3 days with fresh IMDM complete and IL-2 to a final concentration of 1000 IU/ml. After 2-4 weeks, when sufficient T cells were obtained, the cells were cryopreserved and stored in liquid nitrogen until use. Approximately two-third of the tumor pieces was incubated for 15 minutes at 37°C in IMDM dissociation mixture

containing 10% human AB serum, high dose of antibiotics (as above) and 0.38 mg/ml of the commercially available Liberase enzymes (Liberase TL, research grade, Roche). Following incubation, cell suspension was put on a 70 µm cell strainer (Falcon, Durham, NC, USA) to obtain a single cell suspension, counted using trypan blue exclusion (Sigma, St Louis, MO, USA), and cryopreserved at approximately 2 million cells/vial. All cells were stored in the vapor phase of liquid nitrogen until further use.

### **Flow cytometry and data analysis**

Cryopreserved PBMC ( $n=34$ ) and/or cryopreserved freshly isolated single cell tumor samples ( $n=12$ ) were thawed and assessed by flow cytometry as described before.<sup>26, 27</sup> In brief, samples were thawed according to standard operation procedures and stained with the LIVE-DEAD® Fixable yellow dead cell stain kit (ThermoFisher Scientific) for 20 minutes at room temperature to identify dead cells. Following incubation, the cells were washed, incubated with PBS/0.5%BSA/10%FCS for 10minutes on ice to block Fc receptors. After the cells were washed, the cells were stained for 30 minutes on ice and in the dark with fluorochrome-conjugated antibodies. Intracytoplasmic/intranuclear staining was conducted with the BD Pharmingen Transcription Factor Buffer set (BD Biosciences) according to manufacturers' protocol. Details on antibodies used are listed in supplemental table 1. Acquisition of cells was done on a BD LSR Fortessa. Data was analyzed by either manual gating using DIVA software (version 8.02; BD Biosciences) or by high-dimensional single cell data analysis using hierarchical Stochastic Neighbor Embedding (HSNE)<sup>28</sup> in Cytosplore. To automatically discover stratifying biological signatures at the single cell level, we used the fully automated hierarchical clustering (unsupervised) tool CITRUS in the cloud-based cytobank software (Fluidigm Sciences) with an FDR of 1%.

### **Cytokine production of phytohemagglutinin (PHA)-stimulated TIL**

To determine capacity of tumor infiltrating lymphocyte (TIL) batches from HPVnegVSCC tumors to produce cytokines in response to mitogenic stimulation, cultured TIL batches ( $n=14$ ) were stimulated with 0.5 µg/ml PHA (HA16 Remel; ThermoFischer Scientific) for 4 days, after which supernatants were harvested and analyzed by Cytometric Bead Array (CBA, Th1/Th2 kit, BD Bioscience, Breda, the Netherlands) according to the manufacturer's instructions. The cut-off value for cytokine production was 20 pg/ml, except for IFN-γ for which it was 100 pg/ml. Positive cytokine production was defined as at least twice above that of the unstimulated cells.<sup>25, 29</sup>

### **Statistical analysis**

For data analysis the statistical software package SPSS 23.0 (SPSS Inc., Chicago, IL) was used. Group comparisons of categorical data were performed by chi-square test. The non-parametric Mann-Whitney U test was used for continuous variables when comparing two groups. For the survival analysis, patients were categorized into two groups based on

numerical immune cell count. First, the median cell count was used as cut-off value. To optimize the chance to detect a relationship between T cell subsets and clinical outcome in a relatively small group of patients, the best cut-off value for the different T cell subsets was determined using receiver operating characteristics (ROC) curve analysis. The T cell subset values with the best accuracy (i.e., with greatest sensitivity and specificity) were selected as the most optimal cut-off value for (OS or RFP). Based on these cut-off values, the immune cell counts were categorized in two groups and a log-rank test was performed to calculate the difference in OS or RFP. The RFP was censored for lost-to-follow up and death. Two-sided  $p$ -values  $<0.05$  were considered significant. GraphPad Prism 7 (GraphPad Software Inc., LA Jolla, CA, USA) was used to illustrate the data by graphs and figures.

## RESULTS

### Patient cohort

A cohort of 65 primary VSCC samples, divided in HPVpos VSCC ( $n=23$ ), HPVneg/p53wt VSCC ( $n=20$ ), and HPVneg/p53mut VSCC ( $n=22$ ) was analyzed. All cases were matched for age (40-85 years), FIGO stage, absence of lymph node and distant metastasis,  $\geq 8$ mm tumor-free margins, no use of immunosuppression, and no documented medical history. However, HPVpos VSCC were younger than the other groups despite matching because younger women are more likely to have HPVpos VSCC than HPVneg VSCC.<sup>30</sup> An overview of patient characteristics and treatment is given in supplemental table 2. In line with current literature<sup>15, 17, 31</sup>, the group of patients with HPVpos VSCC displayed a better OS and RFP than those with HPVnegVSCC (supplemental figure 1). Furthermore, the recurrence rate increased from HPVpos VSCC (13%), HPVneg/p53wt VSCC (40%) to 59% in HPVneg/p53mut VSCC (supplemental table 2). Together this confirms our selection of a representative cohort of patients for our study.

### The HPVpos VSCCs are most often strongly infiltrated with T cells

The archived tissues sections were simultaneously analyzed for the expression of CD3, CD8, Foxp3, PD-1, and pan-keratin by multispectral immunofluorescence VECTRA analysis, both in the epithelial and stromal compartments (supplemental figure 2). Quantification of the T cells per square mm of tumor revealed that the stroma of VSCC was more densely infiltrated with CD3<sup>+</sup> T cells, CD3<sup>+</sup>CD8<sup>+</sup>Foxp3<sup>-</sup> T cells, CD3<sup>+</sup>CD8<sup>-</sup>Foxp3<sup>+</sup> Tregs, and CD3<sup>+</sup>CD8<sup>+</sup>Foxp3<sup>-</sup> T cells than healthy controls. The number of intraepithelial Tregs was also higher in VSCC (figure 1, supplemental figure 2, supplemental table 3). Comparison of the three subgroups revealed a strong difference in T cell infiltration between HPVpos VSCC and HPVneg/p53mut VSCC. The majority of HPVpos VSCC was well infiltrated whereas the HPVneg/p53mut VSCC most often displayed a low T cell infiltration. The group of HPVneg/p53wt VSCC showed a more variable pattern, with low and high T cell infiltrated tumors (figure 1, supplemental figure 2, supplemental table 3). The number of tumor-infiltrating intraepithelial cells was

highly correlated to the other intraepithelial T cell subsets and to their numbers in the stroma (supplemental table 4). This suggests a coordinated response of CD3<sup>+</sup>CD8<sup>-</sup>Foxp3<sup>-</sup> and CD3<sup>+</sup>CD8<sup>+</sup>Foxp3<sup>-</sup> T cells in VSCC. Quantification of intraepithelial CD3<sup>+</sup>Tbet<sup>+</sup> T cells, representing type 1 immunity<sup>27</sup>, revealed higher numbers in HPVpos VSCC compared to both HPVnegVSCC subtypes (figure 1, supplemental table 3).

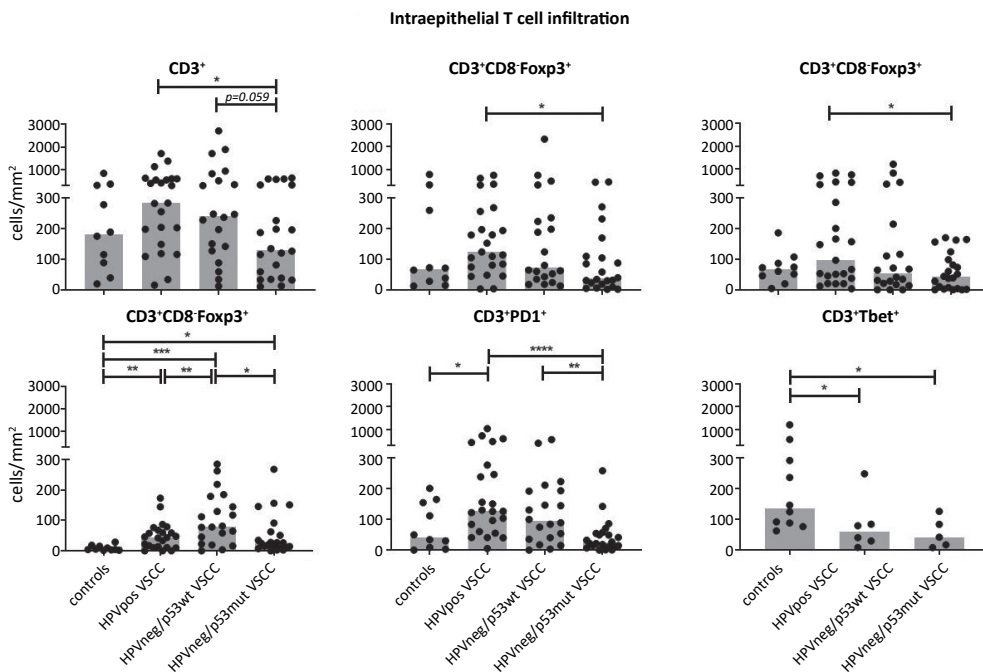


**Figure 1. HPVpos VSCC are highly infiltrated with CD3<sup>+</sup> T cells, especially CD3<sup>+</sup>CD8<sup>-</sup>Foxp3<sup>+</sup> and CD3<sup>+</sup>CD8<sup>+</sup>Foxp3<sup>-</sup> T cells.** The numbers of intraepithelial and stroma infiltrating CD3<sup>+</sup> (T cells), CD3<sup>+</sup>CD8<sup>-</sup>Foxp3<sup>+</sup> (helper T cells), CD3<sup>+</sup>CD8<sup>+</sup>Foxp3<sup>-</sup> (cytotoxic T cells), CD3<sup>+</sup>CD8<sup>-</sup>Foxp3<sup>+</sup> (regulatory T cells) and CD3<sup>+</sup>PD1<sup>+</sup> T cells as cells/mm<sup>2</sup> for HPV-independent healthy labia ( $n=10$ ), and HPVpos VSCC ( $n=23$ ), HPVneg/p53wt VSCC ( $n=20$ ) and HPVneg/p53mut VSCC ( $n=22$ ) patients. CD3<sup>+</sup>Tbet<sup>+</sup> T cells were counted on a subset of the total cohort of 10 HPVpos VSCC, 6 HPVneg/p53wt VSCC and 5 HPVneg/p53mut VSCC. VSCC categorization was based on HPV-PCR, p16-IHC and p53-IHC as described in materials and methods. The bars indicate the median cell count, individual samples are indicated by closed circles. Differences between two groups were calculated with a Mann-Whitney test with the significance indicated with asterisks. \* $p<0.05$ , \*\* $p<0.01$ , \*\*\* $p<0.001$ , and \*\*\*\* $p<0.0001$ .

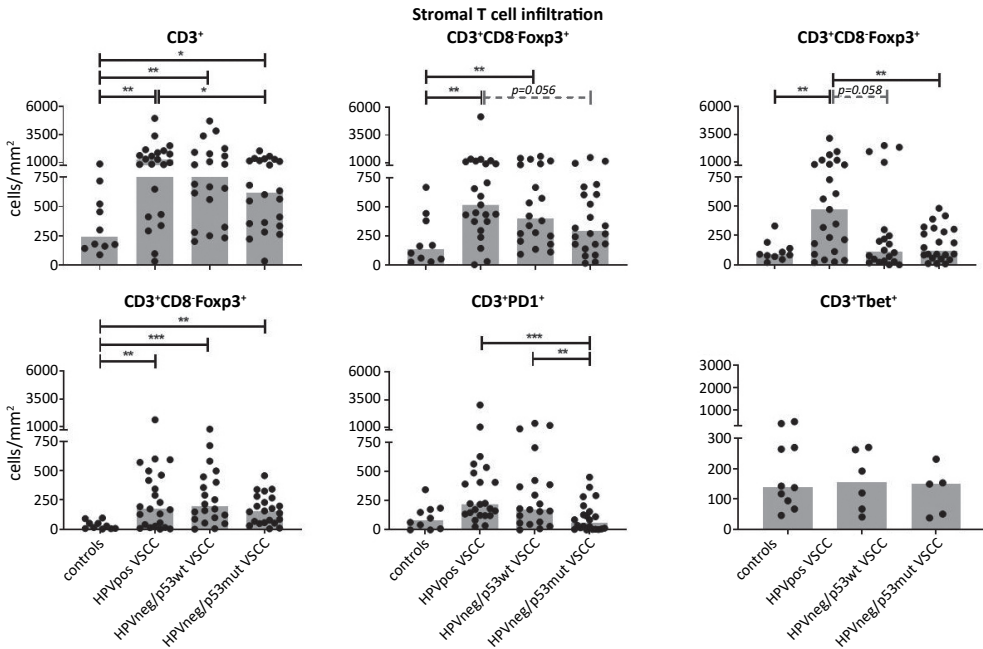
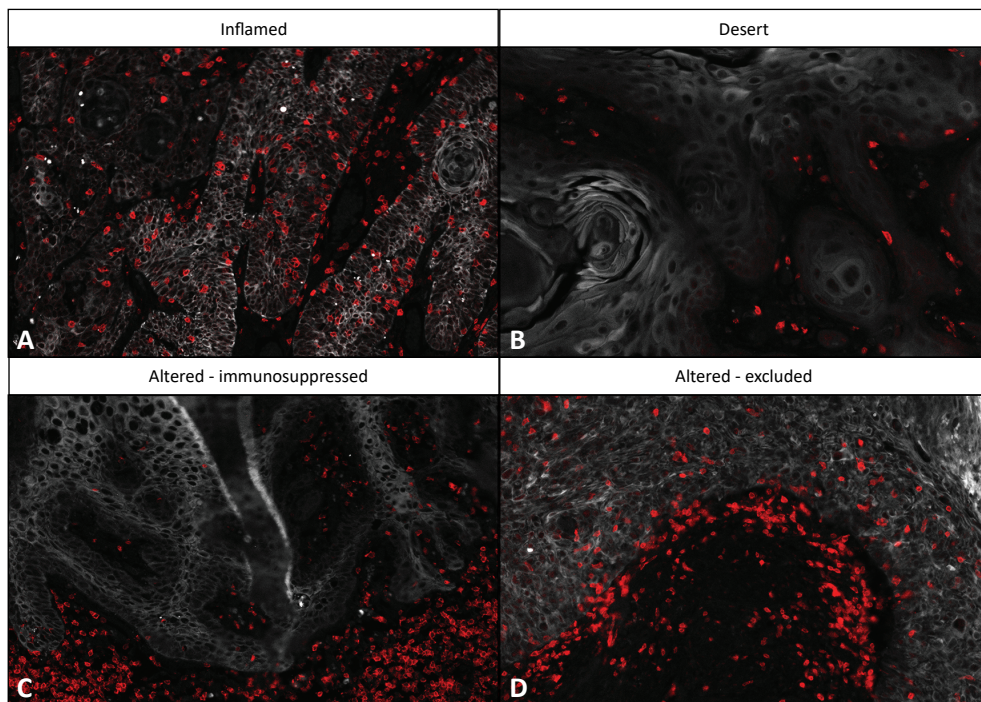


Figure 1. Continued

### Immune inflamed, altered-excluded, altered-immunosuppressed and deserted VSCC.

Based on the previously published categories of T cell infiltration patterns<sup>32</sup>, VSCC were characterized (figure 2), as immune deserted ( $n=19$ ), -altered ( $n=41$ ) or -inflamed ( $n=5$ ). The immune-altered group was the largest and could be subdivided based on two distinct patterns of T cells in the stroma.<sup>33</sup> The altered-excluded tumors ( $n=24$ ) showed more stromal T cells at the invasive border whereas in the altered-immunosuppressed VSCC ( $n=17$ ) T cells were dispersed throughout the whole stroma (figure 2). Notably, the number of CD3<sup>+</sup> T cells at the invasive border (figure 2C) was highly correlated with the intraepithelial CD3<sup>+</sup> T cell count ( $p=0.000$ ; supplemental table 4) in the altered-excluded VSCC. Moreover, the average number of intraepithelial CD3<sup>+</sup> T cells in the altered-excluded was higher than in the altered-immunosuppressed (mean  $612 \pm \text{SD } 539$  vs mean  $157 \pm \text{SD } 92$ ,  $p<0.001$ , respectively). To evaluate the impact of these four VSCC categories on survival, a Kaplan-Meier analysis was performed. The inflamed group displayed a superior RFP and OS (supplemental figure 3). Interestingly, the group of altered-excluded VSCC showed a similar OS whereas the RFP was less good when compared to that of the inflamed group. Therefore, the inflamed and altered-excluded VSCC were classified as hot tumors.



**Figure 2. The T cell infiltration pattern can be used to classify VSCC into four categories.** Categorization of the VSCC based on the pattern of T cell infiltration was done according to literature.<sup>32, 33</sup> Depicted are four representative examples of T cell infiltration patterns: designated immune inflamed (A), deserted (B), altered-immunosuppressed (C), altered-excluded (D). Altered-excluded tumors show more T cells at the invasive border rather than in the middle of the stroma. Red = CD3, white = keratin (epithelial area).

### **The intratumoral CD3<sup>+</sup>CD8<sup>+</sup>Foxp3<sup>-</sup> T cell count is an independent prognostic marker for RFP and OS irrespective of VSCC type**

The better OS of the two categories displaying stronger intraepithelial infiltration than altered-immunosuppressed and deserted VSCC, suggested an important role for intraepithelial T cells on clinical outcome. For each T cell subset, the median cell count (supplemental table 5) and the optimized cut-off point, as determined by ROC curve analysis, was used to categorize the patient's tumor into low or high infiltrated and subsequently its impact on clinical outcome was determined. High intraepithelial infiltration with CD3<sup>+</sup> T cells, in particular of CD3<sup>+</sup>CD8<sup>+</sup>Foxp3<sup>-</sup> T cells was strongly associated with longer RFP ( $p=0.001$ ) and OS ( $p=0.004$ ). A strong infiltration with CD3<sup>+</sup>PD-1<sup>+</sup> T cells was also associated with a longer RFP ( $p=0.032$ ). The intraepithelial infiltration with CD3<sup>+</sup>CD8<sup>+</sup> T cells or CD3<sup>+</sup>CD8<sup>+</sup>Foxp3<sup>+</sup> Tregs was not prognostic for clinical outcome (figure 3, supplemental figure 4). Importantly, the prognostic power of CD3<sup>+</sup>CD8<sup>+</sup>Foxp3<sup>-</sup> T cells for RFP was retained when only the HPVneg VSCC were analyzed (supplemental figure 4). To sustain this notion, the impact of tumor infiltrating CD3<sup>+</sup>CD8<sup>+</sup>Foxp3<sup>-</sup> T cells in clinical outcome was corrected for age, and p53 and HPV status (supplemental table 6). In the univariate analysis, only high CD3<sup>+</sup>CD8<sup>+</sup>Foxp3<sup>-</sup>

counts and age correlated with RFP. In the multivariate analysis, high infiltration with CD3<sup>+</sup>CD8<sup>+</sup>Foxp3<sup>-</sup> T cells but not age was associated with longer RFP (HR=3.30 (95%CI 1.22-8.94),  $p=0.018$ ). Thus, the CD3<sup>+</sup>CD8<sup>+</sup>Foxp3<sup>-</sup> T cell infiltration is expected to be an important prognostic marker for clinical outcome, irrespective of whether these VSCC are caused by the HPV-associated oncogenes or other oncogenic pathways (e.g. *TP53* mutation).

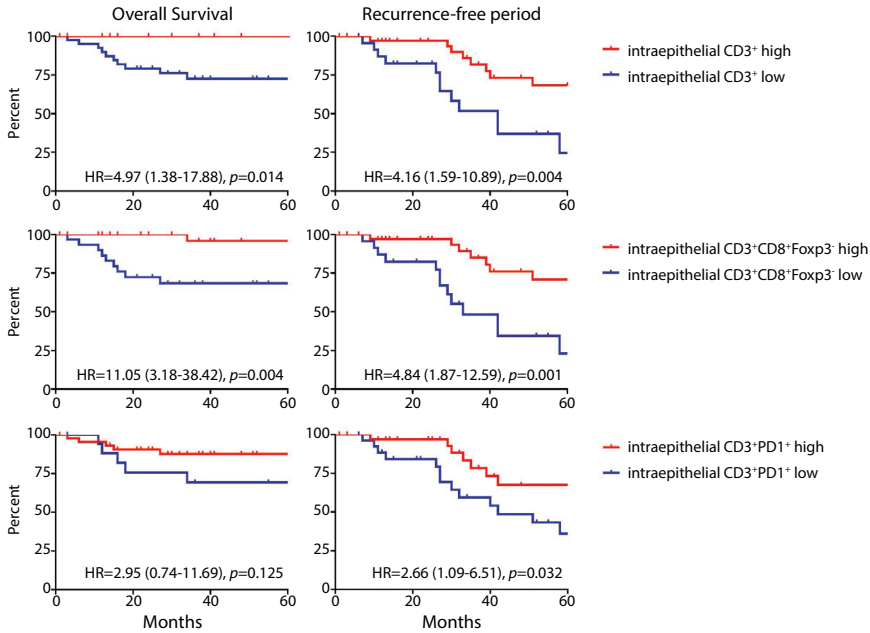
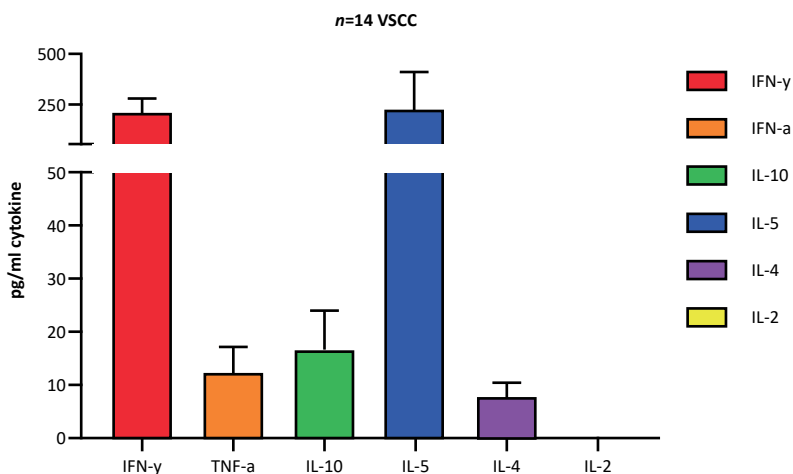


**Figure 3. High numbers of intraepithelial CD3<sup>+</sup> and CD3<sup>+</sup>CD8<sup>+</sup>Foxp3<sup>-</sup> cells are associated with longer overall survival and recurrence-free period.** Kaplan-Meier curves showing overall survival (left) and the recurrence-free period (RFP; right) for VSCC patients with high (red) and low (blue) numbers of intraepithelial CD3<sup>+</sup> (A) and CD3<sup>+</sup>CD8<sup>+</sup>Foxp3<sup>-</sup> (B) and CD3<sup>+</sup>PD1<sup>+</sup> (C) cells/mm<sup>2</sup>. The patients were grouped based on the best cut-off value for each subset as determined by receiver operating characteristics (ROC) curve analysis. The most accurate T cell subset value for either OS or RFP was used. Cut-off values were for CD3<sup>+</sup> T cells 309.4 and 192.7 cells/mm<sup>2</sup> for OS and RFP, respectively, for CD3<sup>+</sup>CD8<sup>+</sup>Foxp3<sup>-</sup> 82.58 and 61.82 cells/mm<sup>2</sup>, and for CD3<sup>+</sup>PD1<sup>+</sup> 37.67 (OS) and 99.96 (RFP) cells/mm<sup>2</sup> for CD3<sup>+</sup>PD1<sup>+</sup> cells, respectively. Patients with a T cell count < cut-off value were classified as low, the others as high. Statistical significance of the survival distribution was analyzed by log-rank testing and significant differences were indicated as \* $p<0.05$ , \*\* $p<0.01$ , \*\*\* $p<0.001$ , and \*\*\*\* $p<0.0001$ .

### HPVneg VSCC are infiltrated by activated CD8<sup>+</sup> and CD4<sup>+</sup> effector memory T cells.

The vast majority (~80%) of vulvar cancers are not induced by HPV.<sup>17</sup> While 78% (18/23) of HPVpos VSCC were strongly infiltrated with CD3<sup>+</sup>CD8<sup>+</sup>Foxp3<sup>-</sup> T cells, there was also a considerable fraction of HPVneg VSCC displaying evidence of their immunogenicity with 60% (12/20) of the HPVneg/p53wt VSCC and 40% (9/22) of the HPVneg/p53mut VSCC showing high intraepithelial CD3<sup>+</sup>CD8<sup>+</sup>Foxp3<sup>-</sup> T cell infiltration and longer RFP and OS. In order to gain a better understanding of these tumor-infiltrating T cells in HPVneg VSCC, a series of fresh HPVneg VSCC tumor biopsies was used to culture tumor-infiltrating lymphocytes (TIL;  $n=14$ ) and for *ex-vivo* phenotypic analysis of freshly dissociated and directly liquid nitrogen stored

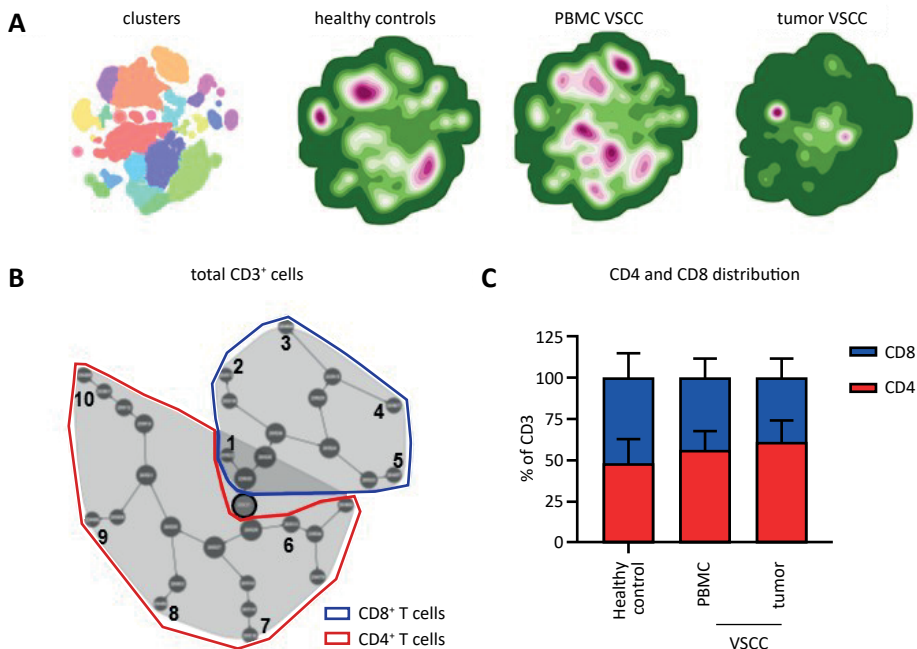
tumor-infiltrating T cells by flow cytometry ( $n=12$ ). Upon mitogenic stimulation, the growing TILs predominantly produced the type 1 cytokine IFN- $\gamma$  and the type 2 cytokine IL-5 at on average similar concentrations, suggesting the presence of both Th1 and Th2 cells in these tumors (figure 4). Only low concentrations of TNF- $\alpha$ , IL-4 and IL-10 were found.



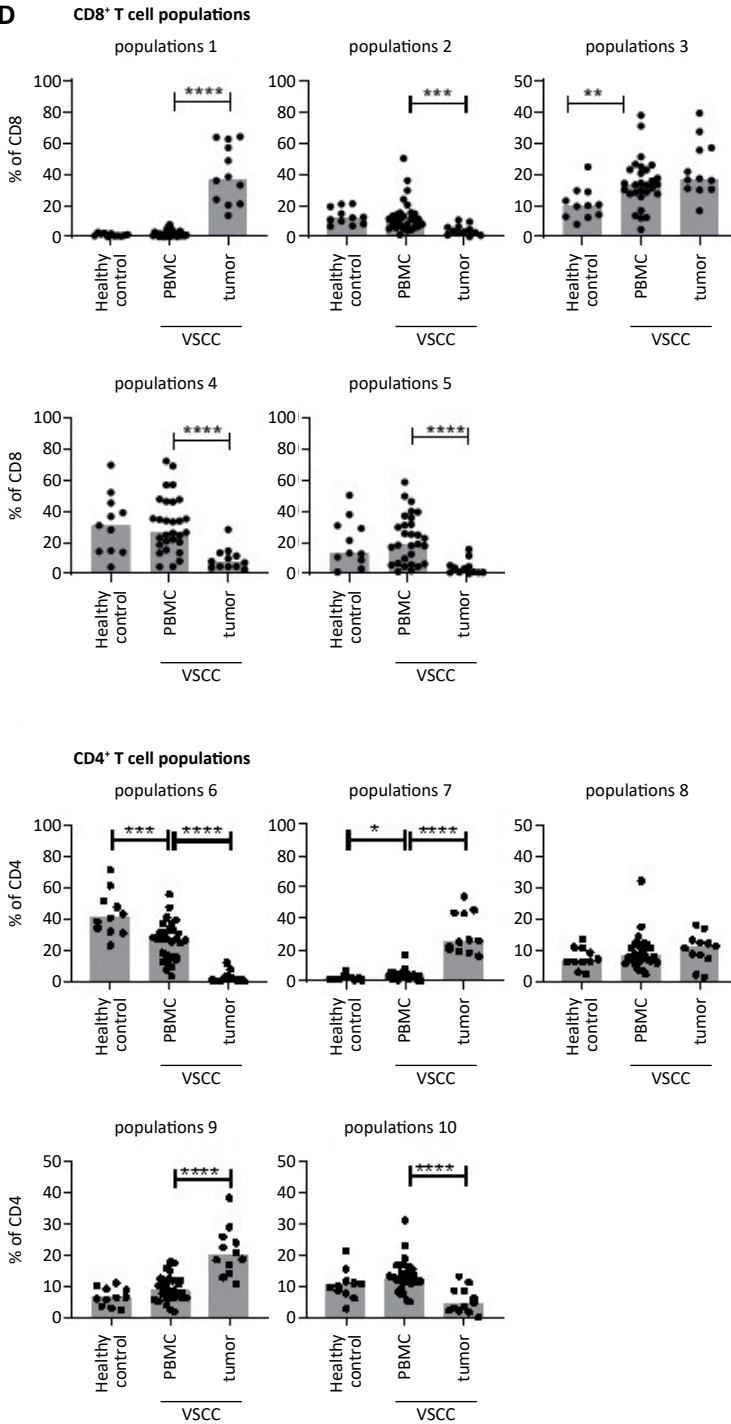
**Figure 4. Tumor-infiltrating lymphocytes produce Th1 and Th2 cytokines upon mitogenic stimulation.** *In vitro* expanded T cells from VSCC were analyzed for their cytokine production following mitogenic stimulation with 0.5  $\mu\text{g/ml}$  PHA for 4 days, after which supernatants were harvested and analyzed by cytometric bead array (CBA) to determine the production of IFN- $\gamma$ , TNF- $\alpha$ , IL-10, IL-5, IL-4 and IL-2 in pg/mL. Mean ( $\pm$  SEM) cytokine production is shown for 14 HPVneg VSCC.

To analyze the tumor-infiltrating T cells an antibody mix against CD45, CD3, CD4, CD8, CCR7, CD45RA, CD103, CD161, PD-1, CD38, HLA-DR and NKG2A was used to stain the fresh VSCC digests. In addition, PBMC of healthy female controls ( $n=11$ ) and PBMC of HPVneg VSCC ( $n=29$ ) were stained. A combined hierarchical Stochastic Neighbor Embedding (HSNE) analysis of the high-dimensional single cell data obtained from staining the blood and tumor samples resulted in the identification of several distinct immune populations (clusters), which were more prominently present or absent in the tumors or PBMC of the VSCC patients (figure 5A). In order to automatically discover stratifying biological signatures within VSCC blood and tumor samples, we made use of the automated and data-driven CITRUS platform, as an unbiased and thorough correlation-based tool for mining and inspection of cell subsets at the single cell level nested within high-dimensional datasets.<sup>34</sup> The CITRUS analysis resulted in ten distinctive (groups of) lymphocyte populations significantly higher present in one or more of the three different types of samples (figure 5B). The CD4 and CD8 distribution within the total CD3<sup>+</sup> T cell population did not differ between PBMC and tumors of VSCC patients (figure 5C). Of the five identified CD8<sup>+</sup> T cell subsets, populations 2, 4, and 5 were significantly underrepresented in VSCC tumors (figure 5D). Population 2 comprised CD8<sup>+</sup>CD161<sup>+</sup>PD-1<sup>+</sup>CD38<sup>+</sup>HLA-DR<sup>-</sup> effector memory RA<sup>+</sup> T cells (Temra), whereas

population 4 (CD8<sup>+</sup> Tcm/em) and population 5 (CD8<sup>+</sup> Temra) did not display these markers (supplemental figure 5). The CD8<sup>+</sup> T cell population (#1) which was clearly overrepresented in VSCC tumors, consisted of CD8<sup>+</sup>CD103<sup>+</sup>CD161<sup>+</sup>NKG2A<sup>+</sup>/PD-1<sup>+</sup>CD38<sup>+</sup>HLA-DR<sup>+</sup> Tem cells. Of the five different CD4<sup>+</sup> T cell subsets identified, population 6 (CD4<sup>+</sup>PD-1<sup>-</sup> CD161<sup>-</sup>CD38<sup>+</sup>HLA-DR<sup>-</sup> naïve T cells) and population 10 (CD4<sup>+</sup>PD-1<sup>-</sup>CD38<sup>-</sup>CD161<sup>-</sup>HLA-DR<sup>-</sup> Tem/cm) were lower in VSCC than PBMC. In contrast, two populations of CD4<sup>+</sup> effector T cells were found at significantly higher percentages and comprised CD4<sup>+</sup>PD-1<sup>+</sup> CD161<sup>-</sup>CD38<sup>+</sup>HLA-DR<sup>+</sup>Tem (#7) as well as CD4<sup>+</sup>PD-1<sup>-</sup> CD161<sup>-</sup>CD38<sup>-</sup>HLA-DR<sup>-</sup>Tcm/em (#9). The co-expression of PD-1, CD38 and HLA-DR is indicative for T cell activation. As such the strong tumor-specific infiltration of HPVnegVSCC with activated CD8<sup>+</sup> (population 1) and CD4<sup>+</sup> (population 7) effector T cells sustains the notion these tumors are immunogenic and explain why their presence is associated with better clinical outcome.



**Figure 5. HPVneg VSCC are infiltrated with highly activated CD4<sup>+</sup> and CD8<sup>+</sup> effector/memory T cells.** PBMC of healthy controls ( $n=11$ ) as well as PBMC ( $n=29$ ) and freshly dissociated tumor-derived TIL ( $n=12$ ) of HPVneg VSCC patients were analyzed by 13-parameter flow cytometry analysis. (A) Hierarchical Stochastic Neighbor Embedding (HSNE) clusters (left) and density plots (right) visualizing the high-dimensional flow cytometry data in two dimensions for the collective total CD3<sup>+</sup> T cells for indicated groups. The identified cell subsets are identified in the cluster plots by the different colors. (B) CITRUS automatic discovery of stratifying biological signatures within tumor and blood samples visualizes 10 distinctive populations of CD8<sup>+</sup> and CD4<sup>+</sup> T cells the total CD3<sup>+</sup> immune population. Every cell population represented by a node is divided on basis of median level of expression of a differently expressed marker into two new nodes (cellular subsets) going from the center (all cells) to the periphery of the plot. (C) The distribution of CD4<sup>+</sup> and CD8<sup>+</sup> T cell frequencies (mean  $\pm$  SEM) within the total CD3<sup>+</sup> T cell population is depicted for healthy control and VSCC PBMC and tumors. (D) Scatter plots with bars displaying frequencies of CD8<sup>+</sup> (# 1 to 5; top panel) and CD4<sup>+</sup> (# 6 to 10; bottom panel) T cell populations are given as % of CD8<sup>+</sup> and CD4<sup>+</sup> cells. \* $p < 0.05$ , \*\* $p < 0.01$ , \*\*\* $p < 0.001$ , and \*\*\*\* $p < 0.0001$ .

**D**

For half (6/12) of the freshly digested VSCC samples enough material was available to characterize the T cell infiltrate with a second antibody mix against CD3, CD4, CD8, CD25, CD127, Foxp3, Tim-3, Lag-3 and Tbet. These samples were analyzed for the presence of different types of Treg, Tbet<sup>+</sup> cells and the two checkpoint molecules according to the strategy shown in supplemental figure 6. Similar to what was found in the FFPE tissue samples, a tumor-specific increase in activated and proliferating (Ki67<sup>+</sup>) Tregs was observed (figure 6A). Furthermore, tumor-specific increases in the percentages of TIM-3 and LAG-3 Tregs, CD8<sup>+</sup> and non-Treg CD4<sup>+</sup> T cells were observed (figure 6B), confirming that part of the tumor-infiltrating T cells has been activated. Last but not least, on average 30% of the CD8<sup>+</sup> and 20% of the non-Treg CD4<sup>+</sup> T cells expressed the transcription factor Tbet, which is in line with the IFN- $\gamma$  production of the cultured TILs. Finally, only a small percentage of the Tregs expressed Tbet (figure 6B). Based on the cytokine production and the expression of several checkpoints, transcription factors and activation markers, we conclude that HPVneg VSCC are infiltrated with variable numbers of activated type 1 and 2 CD8<sup>+</sup> and CD4<sup>+</sup> effector T cells as well as Tregs.

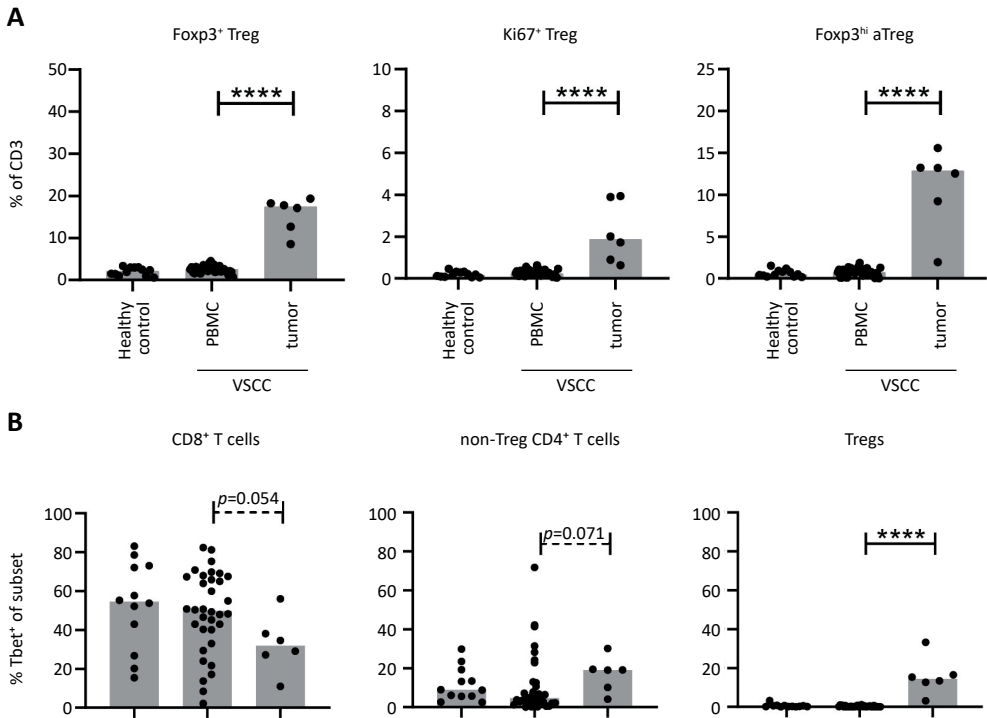


**Figure 6. HPVneg VSCC are infiltrated with activated and Tbet-expressing CD4<sup>+</sup> and CD8<sup>+</sup> T cells and Tregs.** PBMC of healthy controls ( $n=12$ ) and PBMC ( $n=34$ ) and freshly dispersed tumors ( $n=6$ ) of HPVneg VSCC patients were analyzed by 13-parameter flow cytometry analysis. Scatter plots with bars displaying (A) frequencies of total Foxp3<sup>+</sup> Tregs (left) and proliferating (Ki67<sup>+</sup>, middle) and Foxp3<sup>hi</sup> activated Tregs (Foxp3<sup>hi</sup> aTregs, right) within CD3<sup>+</sup> T cells and (B) frequencies of Tbet<sup>+</sup> (top), TIM-3<sup>+</sup> (middle) and LAG-3<sup>+</sup> (bottom) cells within the CD8<sup>+</sup> (left), non-Treg CD4<sup>+</sup> (middle) and Foxp3<sup>+</sup> Treg (right) T cell populations. \* $p<0.05$ , \*\* $p<0.01$ , \*\*\* $p<0.001$ , and \*\*\*\* $p<0.0001$ .

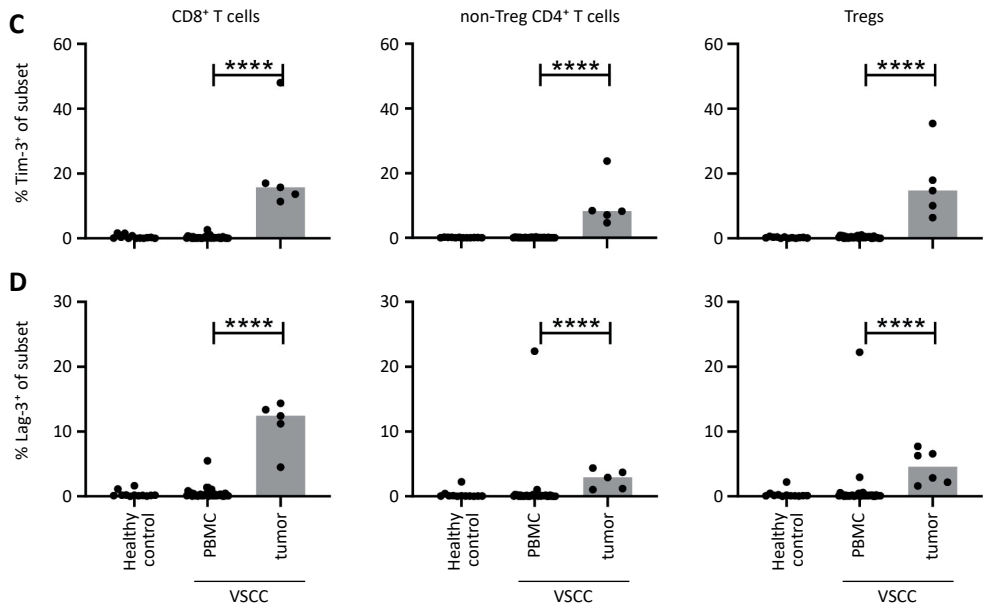


Figure 6. Continued

## DISCUSSION

We asked the question if the observed differences in recurrence rate and survival between the three subtypes of VSCC<sup>14,17</sup>, classified by the presence of HPV, the overexpression of p53 or the absence of both, may have an immunological background. Our study is the first to suggest that a strong infiltration of the tumor cell nests with helper (CD3<sup>+</sup>CD8<sup>+</sup>Foxp3<sup>-</sup>) T cells is important for clinical outcome after primary surgery, irrespective of whether VSCC are caused by HPV or other oncogenic pathways, including *TP53* mutations. Probable reasons for the failure to detect this association in previous studies<sup>6,9-11</sup> are related to the importance of the location of the T cells in the tumor and the homogeneity in stage and treatment of the VSCC patients analyzed. In line with the RFP and the percentage of recurrences found in each of the three subtypes in VSCC, the percentage of tumors with high intraepithelial helper T cell infiltration was the highest in the HPV-associated VSCC (78%), followed by VSCC not associated with HPV or p53 overexpression (60%), and the lowest in VSCC with mutant p53 expression (40%).

Although the helper T cells display the strongest relationship with clinical outcome, this does not mean that CD8<sup>+</sup> T cells are not important in VSCC. Whenever there is a strong intraepithelial infiltration with T cells, this is because both subsets of T cells are present in large numbers. Furthermore, we noted a positive association between the intraepithelial presence of CD3<sup>+</sup>PD-1<sup>+</sup> T cells and clinical outcome. In-depth flow cytometric analysis revealed

that this PD-1<sup>+</sup> T cell population comprised activated CD4<sup>+</sup>PD-1<sup>+</sup>CD161<sup>+</sup>CD38<sup>+</sup>HLA-DR<sup>+</sup> and CD8<sup>+</sup>CD103<sup>+</sup>CD161<sup>+</sup>NKG2A<sup>+</sup>/PD-1<sup>+</sup>CD38<sup>+</sup>HLA-DR<sup>+</sup> effector memory T cells. Potentially, helper T cells play an important role in VSCC because a substantial fraction of VSCC can partially downregulate HLA class I expression whilst the levels of tumor-expressed HLA class II may go up.<sup>35</sup> Based on the percentages of T cells co-expressing the transcription factor Tbet, as counted in the tumor sections and measured in fresh VSCC by flow cytometry, and by the detection of IFN- $\gamma$  and IL-5 in the supernatants of stimulated TIL, the VSCC-infiltrating T cells are both of a type 1 and 2 phenotype.

Current treatment of VSCC does not take into account the differences in etiology and clinical outcome.<sup>3</sup> The relationship between T cell infiltration and clinical outcome suggests that immunotherapy may form a new treatment option for VSCC, as in other tumor types this was associated with a better response to immunotherapy.<sup>32, 33</sup> These other cancer types were categorized into inflamed (hot), - altered (excluded or suppressed) and -deserted (cold) tumors in order to define which immunotherapeutic (combination) approach may work best. For instance, hot tumors show the best response to checkpoint blockade (e.g., anti-PD-1 and anti-CTLA-4).<sup>32, 33</sup> Also VSCC could be divided according to these four immune phenotypes. Only a few (5/65) VSCC were categorized as truly inflamed while a substantial portion (37%,  $n=24$ ) displayed the immune altered-excluded phenotype. However, the latter group displayed a significant stronger intraepithelial T cell infiltration when compared to the immune altered-immunosuppressed phenotype and showed a better OS, hence are also more likely to respond to immunotherapy. The categorization of tumors in hot and cold tumors improves selection of patients that might benefit from immunotherapy such as anti-PD-1 blockade. In our study high percentages of intratumoral T cells expressed PD-1. Others found variable percentages of cases in which the VSCC (>30%) or VSCC-infiltrating immune cells (>90%) expressed PD-L1<sup>11, 36, 37</sup>, congruent with our observation that there are varying numbers of tumor-infiltrating T cells which can produce IFN- $\gamma$ , as indicated by expression of Tbet, and may lead to adaptive PD-L1 expression.<sup>38</sup> Altogether, this makes a strong case for the treatment of a substantial portion of VSCC tumors with PD-1/PD-L1 checkpoint therapy. Indeed, a first successfully treated case with advanced stage recurrent vulvar cancer has been reported with PD-L1 blockade.<sup>39</sup> A tumor-specific increase of the CD4<sup>+</sup> T cell response seems more likely to be achieved by CTLA4-blockade than by targeting PD-1<sup>40</sup>, arguing for a combination of PD-L1 and CTLA-4 blockade to reinvigorate the tumor-specific CD4<sup>+</sup> T cell response. Another option would be the use of an agonistic antibody to OX-40<sup>41</sup>, which in combination with PD-L1 blockade displayed synergistic effects on CD4<sup>+</sup> T cell reactivity.<sup>40</sup>

One-third of our VSCC were phenotyped as deserted or cold tumors which may exist because of a lack of antigens or their presentation (immune ignorance), or because of several deficits leading to a lack of priming or to tolerance.<sup>32</sup> Apart from the HPV-associated VSCC, 40-60% of the HPVneg VSCC display strong intraepithelial T cell infiltration, suggesting that also in

these tumors immunogenic tumor antigens are expressed and presented. Currently, the antigens recognized by T cells in HPVneg VSCC are unknown but the majority of primary VSCC express for instance the well-known tumor antigens MAGEA1 and MAGEA4<sup>42</sup>, but it is unknown if these antigens function as target for the VSCC-infiltrating and still needs to be studied. More likely, a lack of inflammation or danger signals has played a role in HPVneg VSCC. Intratumoral activation of the Stimulator of Interferon Genes (STING) pathway<sup>43</sup>, the use of oncolytic viruses<sup>44</sup>, but also intratumoral injections of toll-like receptor (TLR)-agonists<sup>45</sup> have been shown to sensitize cold tumors to checkpoint blockade. For cold VSCC tumors, the TLR7/8-agonist imiquimod may be a promising topically applied therapeutic agent. Imiquimod elevates numerous genes involved in the regulation of innate immunity, resulting in the migration of DC to the application site, and subsequently the activation of a type 1 T cell response.<sup>46</sup> Patients with a precancerous lesion of HPVpos VSCC responded very well to imiquimod therapy.<sup>47</sup> Notably, imiquimod treatment of breast metastases in the skin not only converted them from cold to hot, as demonstrated by a profound infiltration with CD4<sup>+</sup> and CD8<sup>+</sup> T cells, but also led to tumor regression.<sup>48</sup> Moreover, HPVpos VSCC could benefit from SLP-HPV16 vaccination as shown in HPV-driven oropharyngeal cancers.<sup>24</sup> However, the immune response on this vaccination in VSCC needs to be studied. There are several limitations to our study. The correlation between better clinical outcome and intraepithelial T cell infiltration was found in a highly homogeneous patient group with early-stage cancer and treated with surgery. If this relationship also exists in locally advanced cancer patients treated with (chemo)radiotherapy has to be determined. Furthermore, next to the median cell count, we optimized the chance to detect a statistically significant relation between T cell subsets and clinical outcome in a relatively small group of patients. Hence our results need to be validated in a larger cohort. In addition, our data suggests that the etiology of the VSCC may have an impact on its immunogenicity. While this would fit with the concept that different oncogenic pathways may influence local immunity<sup>18, 19</sup>, the numbers of VSCC analyzed are such that the outcome can only be used for hypothesis generation. Moreover, we have not analyzed the myeloid cell component, which on itself may impact prognosis and T cell function. Finally, less than 20% of VSCC are induced by HPV. As such, we merely collected small pieces of fresh tumor tissue and PBMCs from HPVneg VSCC patients. A more extensive comparison of the tumor-infiltrating immune phenotypes between HPV-associated and HPVneg VSCC, therefore, was not possible.

In conclusion, our observation that a strong coordinated intraepithelial infiltration with T cells is highly associated with a better clinical course of early stage VSCC after surgery and suggests that this group of patients may benefit from immunotherapy as an alternative to potential mutilating surgery in this delicate anatomical area.<sup>3</sup> In parallel to the use of the different categories of immune cell infiltrated tumors in other types of cancer<sup>32, 33</sup>, these tumor classifications can also be used to tailor immunotherapy approaches in VSCC. Near future studies should focus on the effects of checkpoint blockade in patients classified with

inflamed and altered-excluded tumors while patients diagnosed with a deserted (cold) VSCC may benefit more from therapies that induce acute inflammation. Furthermore, future studies should assess the mutational landscape of VSCC as this will reveal if a tumor-specific (neo)-antigen T cell repertoire could be harnessed to treat the HPVneg VSCC.

## **ACKNOWLEDGEMENTS**

We gratefully thank all the patients and healthy individuals who participated in this study. Furthermore, Sandra van den Broek-Veldstra and Margriet Löwik for including the patients in the Circle study. This study was financially supported by grants from the Dutch Cancer Society 2016-10168 to MIEvP, TB, and SHvdB

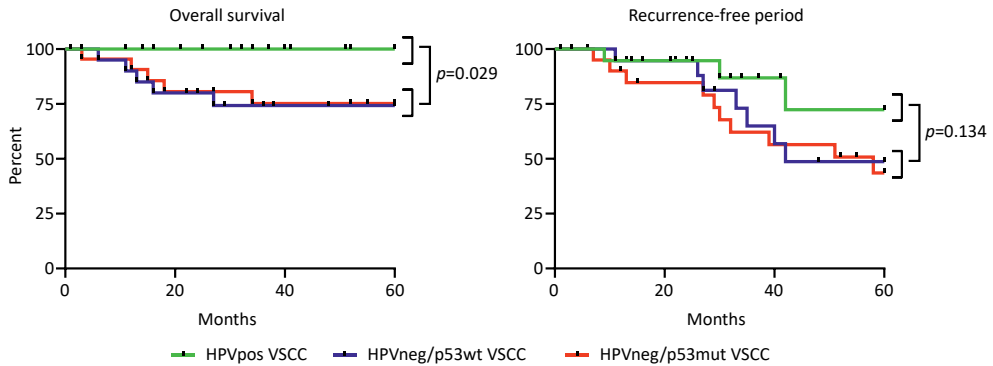
## REFERENCES

1. Mellman, I., et al., *De-Risking Immunotherapy: Report of a Consensus Workshop of the Cancer Immunotherapy Consortium of the Cancer Research Institute*. *Cancer Immunol Res*, 2016. 4(4): p. 279-88.
2. van der Velden, J., G. Fons, and T.A. Lawrie, *Primary groin irradiation versus primary groin surgery for early vulvar cancer*. *Cochrane Database Syst Rev*, 2011(5): p. Cd002224.
3. Gaarenstroom, K., et al., *Postoperative complications after vulvectomy and inguinofemoral lymphadenectomy using separate groin incisions*. 2003. 13(4): p. 522-527.
4. Te Grootenhuys, N.C., et al., *Prognostic factors for local recurrence of squamous cell carcinoma of the vulva: A systematic review*. *Gynecol Oncol*, 2017.
5. Raspollini, M.R., G. Asirelli, and G.L. Taddei, *Analysis of lymphocytic infiltrate does not help in prediction of vulvar squamous cell carcinoma arising in a background of lichen sclerosus*. *Int J Gynaecol Obstet*, 2008. 100(2): p. 190-1.
6. Sznurkowski, J.J., et al., *Prognostic significance of CD4+ and CD8+ T cell infiltration within cancer cell nests in vulvar squamous cell carcinoma*. *Int J Gynecol Cancer*, 2011. 21(4): p. 717-21.
7. van Esch, E.M., et al., *Expression of coinhibitory receptors on T cells in the microenvironment of usual vulvar intraepithelial neoplasia is related to proinflammatory effector T cells and an increased recurrence-free survival*. *Int J Cancer*, 2015. 136(4): p. E95-106.
8. van Esch, E.M., et al., *Intraepithelial macrophage infiltration is related to a high number of regulatory T cells and promotes a progressive course of HPV-induced vulvar neoplasia*. *Int J Cancer*, 2015. 136(4): p. E85-94.
9. de Jong, R.A., et al., *Status of cellular immunity lacks prognostic significance in vulvar squamous carcinoma*. *Gynecol Oncol*, 2012. 125(1): p. 186-93.
10. Sznurkowski, J.J., et al., *Expression of indoleamine 2,3-dioxygenase predicts shorter survival in patients with vulvar squamous cell carcinoma (vSCC) not influencing on the recruitment of FOXP3-expressing regulatory T cells in cancer nests*. *Gynecol Oncol*, 2011. 122(2): p. 307-12.
11. Hecking, T., et al., *Tumoral PD-L1 expression defines a subgroup of poor-prognosis vulvar carcinomas with non-viral etiology*. *Oncotarget*, 2017. 8(54): p. 92890-92903.
12. Taube, J.M., et al., *Colocalization of inflammatory response with B7-h1 expression in human melanocytic lesions supports an adaptive resistance mechanism of immune escape*. *Sci Transl Med*, 2012. 4(127): p. 127ra37.
13. Sznurkowski, J.J., A. Zawrocki, and W. Biernat, *Subtypes of cytotoxic lymphocytes and natural killer cells infiltrating cancer nests correlate with prognosis in patients with vulvar squamous cell carcinoma*. *Cancer Immunol Immunother*, 2014. 63(3): p. 297-303.
14. Nooij, L.S., et al., *Genomic Characterization of Vulvar (Pre)cancers Identifies Distinct Molecular Subtypes with Prognostic Significance*. *Clin Cancer Res*, 2017. 23(22): p. 6781-6789.
15. van de Nieuwenhof, H.P., et al., *The etiologic role of HPV in vulvar squamous cell carcinoma fine tuned*. *Cancer Epidemiol Biomarkers Prev*, 2009. 18(7): p. 2061-7.

16. Dong, F., et al., *Squamous Cell Carcinoma of the Vulva: A Subclassification of 97 Cases by Clinicopathologic, Immunohistochemical, and Molecular Features (p16, p53, and EGFR)*. *Am J Surg Pathol*, 2015. 39(8): p. 1045-53.
17. Hinten, F., et al., *Vulvar cancer: Two pathways with different localization and prognosis*. *Gynecol Oncol*, 2018. 149(2): p. 310-317.
18. Spranger, S., R. Bao, and T.F. Gajewski, *Melanoma-intrinsic beta-catenin signalling prevents anti-tumour immunity*. *Nature*, 2015. 523(7559): p. 231-5.
19. Peng, W., J.A. McKenzie, and P. Hwu, *Complementing T-cell Function: An Inhibitory Role of the Complement System in T-cell-Mediated Antitumor Immunity*. *Cancer Discov*, 2016. 6(9): p. 953-5.
20. de Sanjose, S., et al., *Worldwide human papillomavirus genotype attribution in over 2000 cases of intraepithelial and invasive lesions of the vulva*. *Eur J Cancer*, 2013. 49(16): p. 3450-61.
21. Piersma, S.J., et al., *Human papilloma virus specific T cells infiltrating cervical cancer and draining lymph nodes show remarkably frequent use of HLA-DQ and -DP as a restriction element*. *Int J Cancer*, 2008. 122(3): p. 486-94.
22. de Vos van Steenwijk, P.J., et al., *An unexpectedly large polyclonal repertoire of HPV-specific T cells is poised for action in patients with cervical cancer*. *Cancer Res*, 2010. 70(7): p. 2707-17.
23. Ijsselsteijn, M.E., et al., *Cancer immunophenotyping by 7 colour multispectral imaging without tyramide signal amplification*. *J Pathol Clin Res*, 2018.
24. Welters, M.J.P., et al., *Intratatumoral HPV16-Specific T Cells Constitute a Type I-Oriented Tumor Microenvironment to Improve Survival in HPV16-Driven Oropharyngeal Cancer*. *Clin Cancer Res*, 2018. 24(3): p. 634-647.
25. Santegoets, S.J., et al., *The Anatomical Location Shapes the Immune Infiltrate in Tumors of Same Etiology and Affects Survival*. *Clin Cancer Res*, 2018.
26. Santegoets, S.J., et al., *Monitoring regulatory T cells in clinical samples: consensus on an essential marker set and gating strategy for regulatory T cell analysis by flow cytometry*. *Cancer Immunol Immunother*, 2015. 64(10): p. 1271-86.
27. Santegoets, S.J., et al., *Tbet-positive regulatory T cells accumulate in oropharyngeal cancers with ongoing tumor-specific type 1 T cell responses*. *J Immunother Cancer*, 2019. 7(1): p. 14.
28. Pezzotti N, H.T., Lelieveldt B, Eisemann E, Vilanova A., *Hierarchical Stochastic Neighbor Embedding*. *Compt. Graph. Forum*, 2016. 35: p. 21-30.
29. Welters, M.J.P., et al., *Intratatumoral HPV16-specific T-cells constitute a type 1 oriented tumor microenvironment to improve survival in HPV16-driven oropharyngeal cancer*. *Clin Cancer Res*, 2017.
30. Rumbold, A.R., et al., *Investigating a cluster of vulvar cancer in young women: a cross-sectional study of genital human papillomavirus prevalence*. *BMC Infect Dis*, 2012. 12: p. 243.
31. Monk, B.J., et al., *Prognostic significance of human papillomavirus DNA in vulvar carcinoma*. *Obstet Gynecol*, 1995. 85(5 Pt 1): p. 709-15.
32. Chen, D.S. and I. Mellman, *Elements of cancer immunity and the cancer-immune set point*. *Nature*, 2017. 541(7637): p. 321-330.

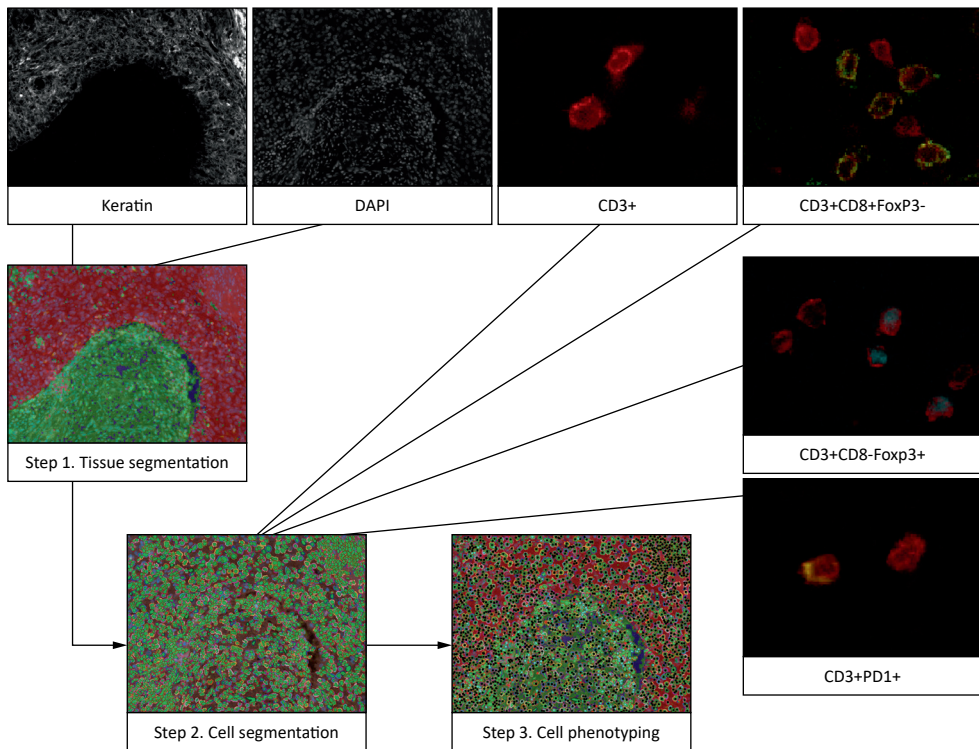
33. Galon, J. and D. Bruni, *Approaches to treat immune hot, altered and cold tumours with combination immunotherapies*. Nat Rev Drug Discov, 2019. 18(3): p. 197-218.
34. Bruggner, R.V., et al., *Automated identification of stratifying signatures in cellular subpopulations*. Proc Natl Acad Sci U S A, 2014. 111(26): p. E2770-7.
35. van Esch, E.M., et al., *Alterations in classical and nonclassical HLA expression in recurrent and progressive HPV-induced usual vulvar intraepithelial neoplasia and implications for immunotherapy*. Int J Cancer, 2014. 135(4): p. 830-42.
36. Howitt, B.E., et al., *Genetic Basis for PD-L1 Expression in Squamous Cell Carcinomas of the Cervix and Vulva*. JAMA Oncol, 2016. 2(4): p. 518-22.
37. Thangarajah, F., et al., *Clinical impact of PD-L1 and PD-1 expression in squamous cell cancer of the vulva*. J Cancer Res Clin Oncol, 2019. 145(6): p. 1651-1660.
38. Garcia-Diaz, A., et al., *Interferon Receptor Signaling Pathways Regulating PD-L1 and PD-L2 Expression*. Cell Rep, 2017. 19(6): p. 1189-1201.
39. Shields, L.B.E. and M.E. Gordinier, *Pembrolizumab in Recurrent Squamous Cell Carcinoma of the Vulva: Case Report and Review of the Literature*. Gynecol Obstet Invest, 2018: p. 1-5.
40. Wei, S.C., et al., *Distinct Cellular Mechanisms Underlie Anti-CTLA-4 and Anti-PD-1 Checkpoint Blockade*. Cell, 2017. 170(6): p. 1120-1133.e17.
41. Hirschhorn-Cymerman, D., et al., *Induction of tumoricidal function in CD4+ T cells is associated with concomitant memory and terminally differentiated phenotype*. J Exp Med, 2012. 209(11): p. 2113-26.
42. Sznurkowski, J.J., et al., *Should we consider cancer/testis antigens NY-ESO-1, MAGE-A4 and MAGE-A1 as potential targets for immunotherapy in vulvar squamous cell carcinoma?* Histopathology, 2011. 58(3): p. 481-3.
43. Corrales, L., et al., *The host STING pathway at the interface of cancer and immunity*. J Clin Invest, 2016. 126(7): p. 2404-11.
44. Bourgeois-Daigneault, M.C., et al., *Neoadjuvant oncolytic virotherapy before surgery sensitizes triple-negative breast cancer to immune checkpoint therapy*. Sci Transl Med, 2018. 10(422).
45. Sato-Kaneko, F., et al., *Combination immunotherapy with TLR agonists and checkpoint inhibitors suppresses head and neck cancer*. JCI Insight, 2017. 2(18).
46. Schon, M.P. and M. Schon, *Imiquimod: mode of action*. Br J Dermatol, 2007. 157 Suppl 2: p. 8-13.
47. van Seters, M., et al., *Treatment of vulvar intraepithelial neoplasia with topical imiquimod*. N Engl J Med, 2008. 358(14): p. 1465-73.
48. Adams, S., et al., *Topical TLR7 agonist imiquimod can induce immune-mediated rejection of skin metastases in patients with breast cancer*. Clin Cancer Res, 2012. 18(24): p. 6748-57.

## SUPPLEMENTAL MATERIALS



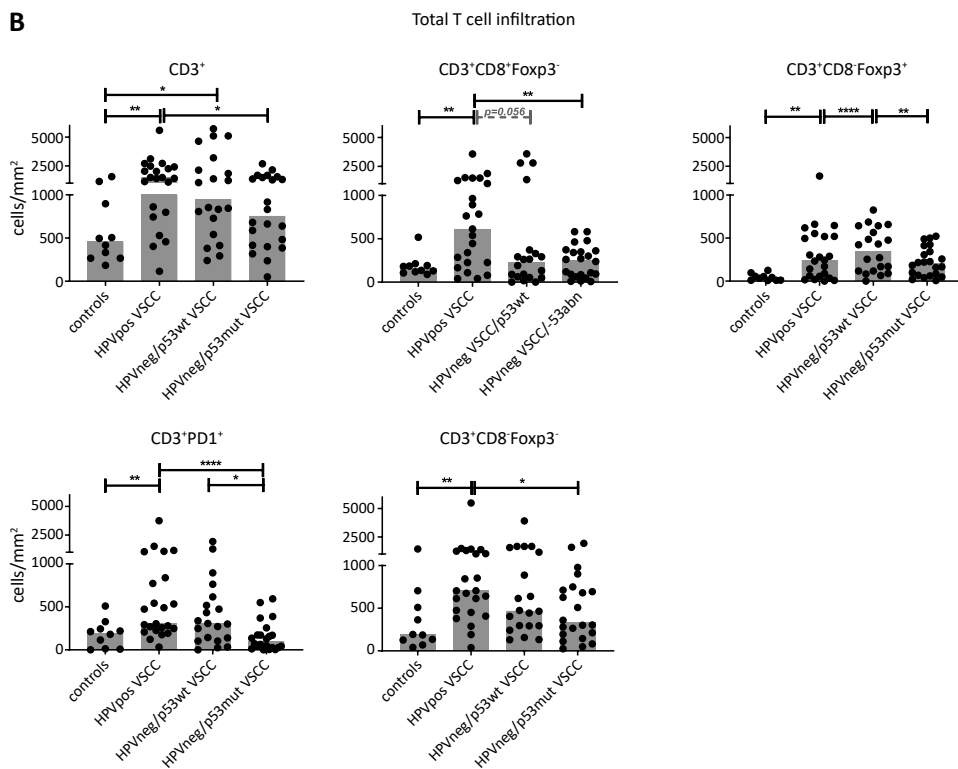
**Supplemental figure 1. HPVpos VSCC have better overall survival compared to HPVneg VSCC.** Kaplan-Meier curves showing overall survival (left) and the recurrence free period (RFP, right) for VSCC patients with HPVposVSCC (green), HPVneg/p53wt VSCC (blue) and HPVneg/p53mut VSCC (red). Statistical significance of the survival distribution was analyzed by log-rank testing. Significant differences between the overall survival of HPVpos VSCC and HPVneg/p53wt VSCC (HR=0.14 (95%CI 0.02-0.80),  $p=0.03$ ) or HPVneg/p53mut VSCC (HR=0.15 (95%CI 0.03-0.87),  $p=0.04$ ) is observed. Comparison of the RFP showed similar differences between the groups. HPVpos VSCC have better clinical outcome than HPVneg/p53wt VSCC (HR=0.48 (95%CI 0.14-1.60),  $p=0.25$ ) and HPVneg/p53mut VSCC (HR=0.41 (95%CI 0.14-1.24),  $p=0.11$ ).

A

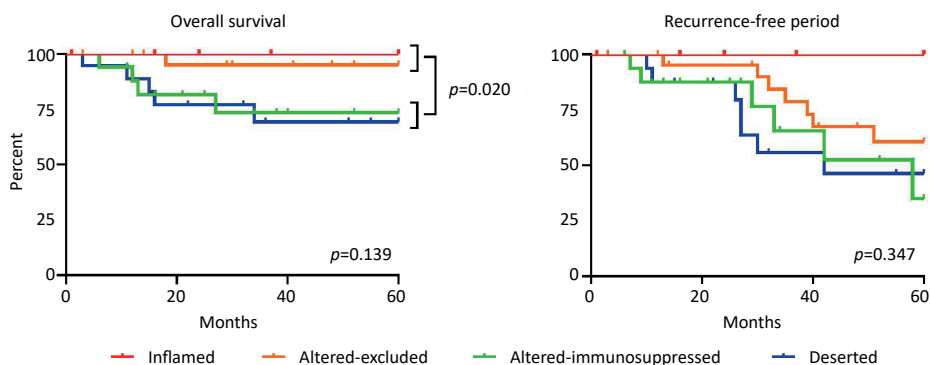


**Supplemental figure 2. Tissue segmentation and image analysis by VECTRA and total T cell infiltrate in VSCC subtypes and healthy controls.** (A) Imaging analysis and spectral separation of dyes was performed with the InForm Cell Analysis software (Perkin Elmer) by using spectral libraries defined with single-marker immunofluorescence detection. All images were segmented into tumor, stroma, and 'no tissue' areas with manual training based on keratin and DAPI. Subsequently, cellular segmentation was performed using counterstain-based approach with DAPI to segment membrane markers (CD3, CD8, and PD1) and nuclei markers (Foxp3). The notorious autofluorescence of erythrocytes was excluded by the absence of DAPI. The phenotype training (CD3<sup>+</sup> total, CD3<sup>+</sup>CD8<sup>+</sup>Foxp3<sup>-</sup>, CD3<sup>+</sup>CD8<sup>+</sup>Foxp3<sup>+</sup>, CD3<sup>+</sup>CD8<sup>-</sup>Foxp3<sup>+</sup>) was done semi-automatically after manual training per tumor where at least 20 cells per phenotype were defined. CD3<sup>+</sup>PD1<sup>+</sup> phenotype was analyzed in a separate training session.

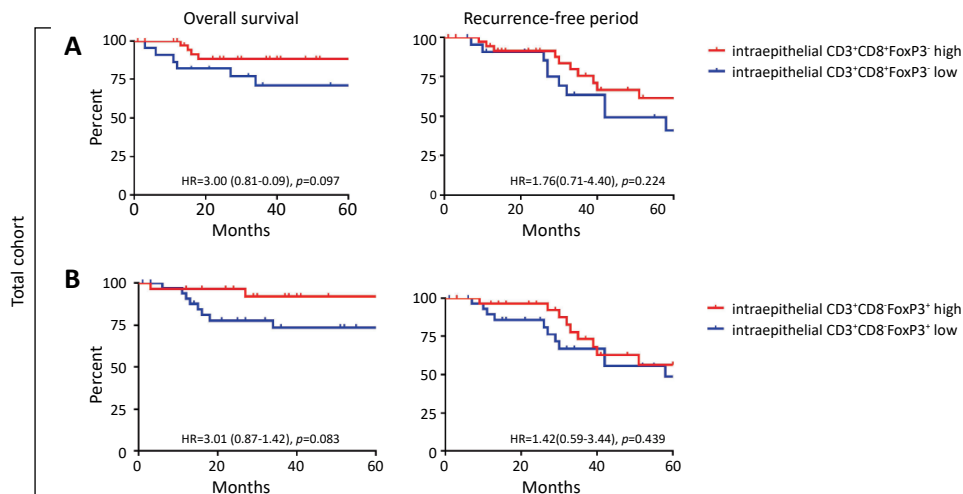
A group of 65 archived tissues sections from VSCC patients and 10 labia from healthy women were simultaneously analyzed for the expression of CD3, CD8, Foxp3, PD-1, and pan-keratin as described above (B). The total number of intraepithelial and stroma infiltrating CD3 (T cells), CD3<sup>+</sup>CD8<sup>+</sup>Foxp3<sup>-</sup> (helper T cells), CD3<sup>+</sup>CD8<sup>+</sup>Foxp3<sup>+</sup> (cytotoxic T cells), CD3<sup>+</sup>CD8<sup>-</sup>Foxp3<sup>+</sup> (regulatory T cells) and CD3<sup>+</sup>PD1<sup>+</sup> T cells are given as cells/mm<sup>2</sup> for HPV-independent healthy labia ( $n=10$ ), and HPVposVSCC, HPVneg/p53wt and HPVneg/p53mut VSCC patients ( $n=23$ ,  $n=20$  and  $n=22$  respectively, B). A sub-cohort was analyzed for the CD3<sup>+</sup>Tbet<sup>+</sup> T cells in 10 HPVpos VSCC, 6 HPVneg/p53wt VSCC and 5 HPVneg/p53mut VSCC. The bars indicate the median cell count, individual samples are indicated by closed circles. Differences between two groups were calculated with a Mann-Whitney test with the significance indicated with asterisks. \* $p<0.05$ , \*\* $p<0.01$ , \*\*\* $p<0.001$ , and \*\*\*\* $p<0.0001$ .

**B**

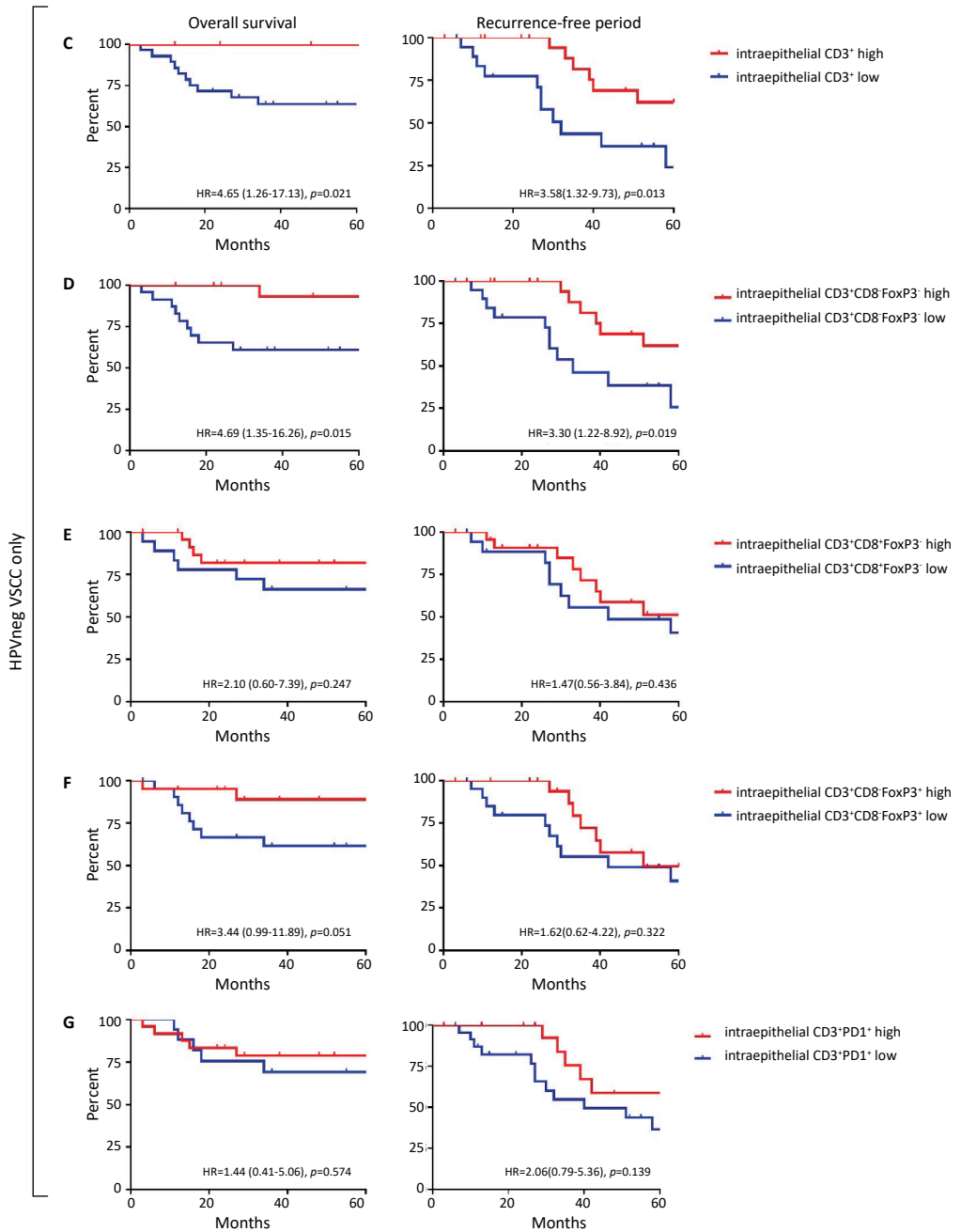
Supplemental figure 2. Continued



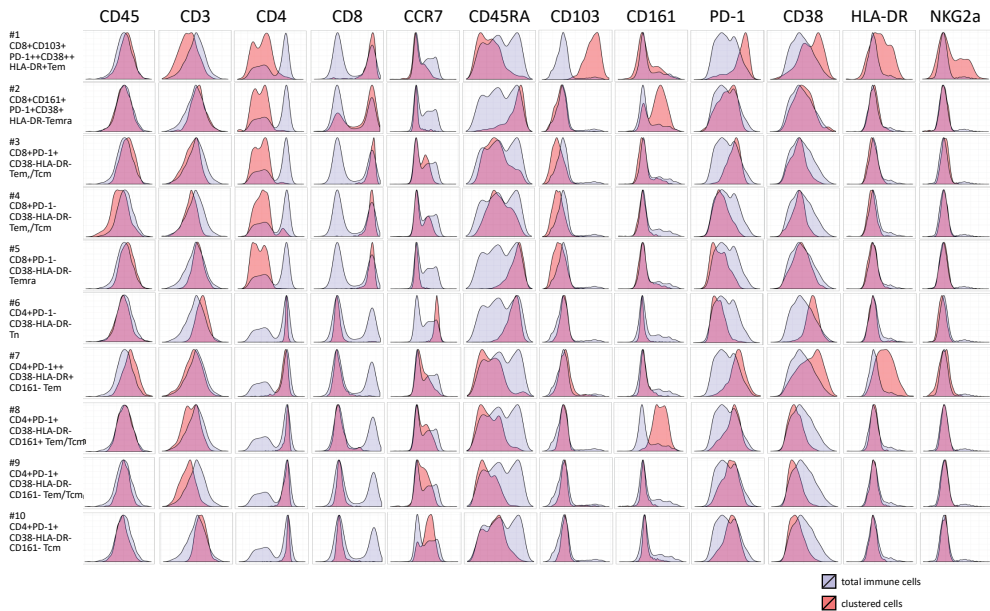
**Supplemental figure 3. Differences in survival for the four immune categories of VSCC.** Kaplan-Meier curves showing overall survival (left) and the recurrence free period (RFP, right) for VSCC patients with inflamed (red,  $n=5$ ), altered-excluded (orange,  $n=24$ ), altered-immunosuppressed (green,  $n=17$ ) and deserted (blue,  $n=19$ ) T cell infiltration patterns. Statistical significance of the survival distribution was analyzed by log-rank testing, and differences were considered significant when  $p < 0.05$ . Although the difference between the four groups is not statistically significant, the combined group of inflamed with altered-excluded displayed longer overall survival ( $p=0.02$ ) than the combined group of patients with altered-immunosuppressed and deserted VSCC.



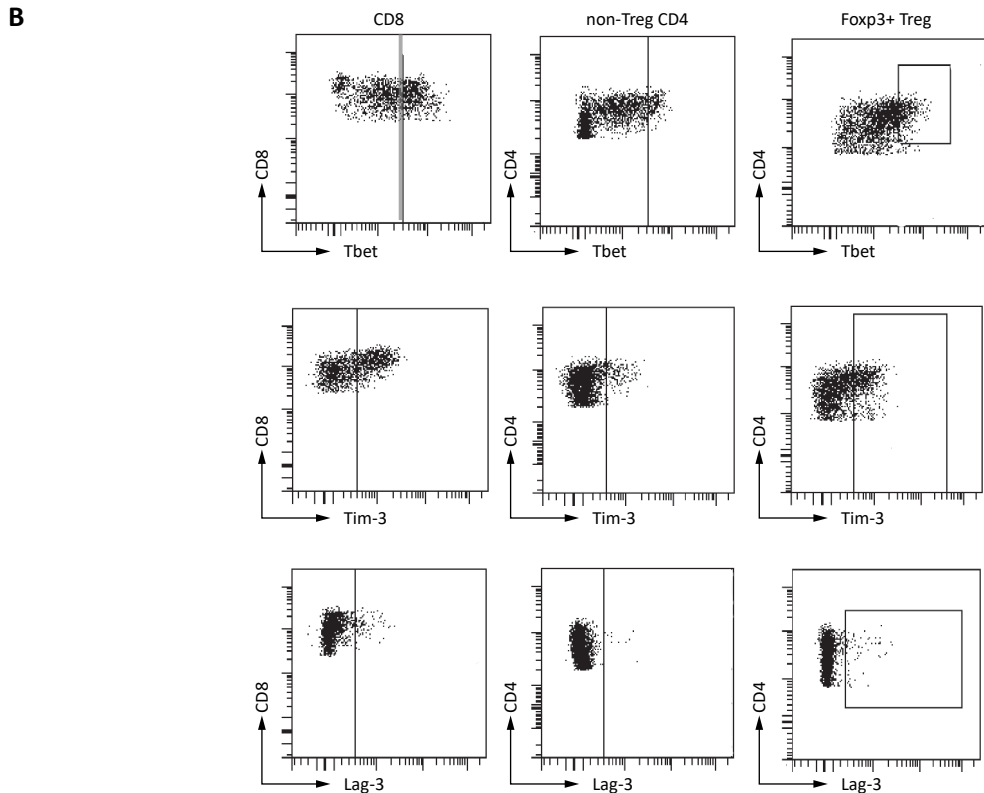
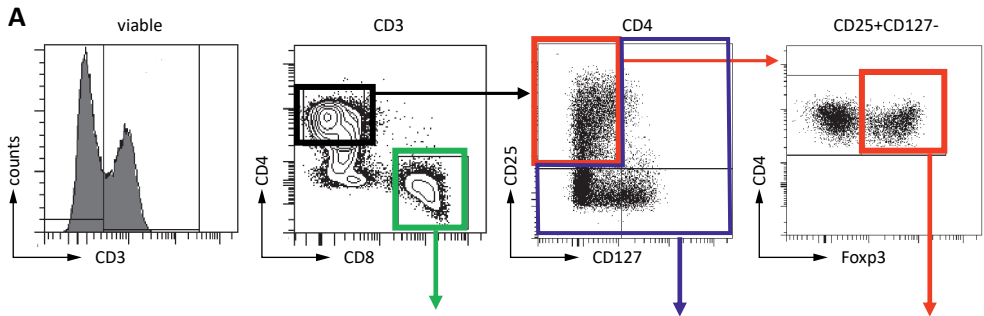
**Supplemental figure 4. Clinical impact of several subsets of intraepithelial T cells in the total group of VSCC and in HPVneg VSCC patients only.** Kaplan-Meier curves showing overall survival (left) and the recurrence free period (RFP, right) for VSCC patients with high (in red) and low (in blue) numbers of intraepithelial CD3<sup>+</sup>CD8<sup>+</sup>Foxp3<sup>+</sup> (A) and intraepithelial CD3<sup>+</sup>CD8<sup>+</sup>Foxp3<sup>+</sup> cells/mm<sup>2</sup> (B). Moreover, we calculated the impact of T-cell phenotypes on HPVneg VSCC only ( $n=42$ , C-G) on clinical outcome. This showed that intraepithelial CD3<sup>+</sup> (panel C), CD3<sup>+</sup>CD8<sup>+</sup>Foxp3<sup>+</sup> T cells (D) retained their positive association with OS and RFP. While other phenotypes in HPVneg VSCC (E-G) were not associated with better clinical outcome. Patients were grouped into the high or low groups based on the best cut-off value for each subset as determined by receiver operating characteristics (ROC) curve analysis. Cut-off values for the total cohort and HPVneg VSCC were similar (CD3<sup>+</sup> cells were 309.4 cells/mm<sup>2</sup> and 192.7 cells/mm<sup>2</sup> for OS and RFP, respectively). The value of cells/mm<sup>2</sup> were for CD3<sup>+</sup>CD8<sup>+</sup>Foxp3<sup>+</sup> cells 35.63 (OS) and 37.96 (RFP), for CD3<sup>+</sup>CD8<sup>+</sup>Foxp3<sup>+</sup> cells 82.58 (OS) and 61.82 (RFP), for CD3<sup>+</sup>CD8<sup>+</sup>Foxp3<sup>+</sup> cells were 35.63 (OS) and 37.96 (RFP), for CD3<sup>+</sup>CD8<sup>+</sup>Foxp3<sup>+</sup> cells 54.58 (OS) and 38.71 (RFP), and for CD3<sup>+</sup>PD1<sup>+</sup> 37.67 (OS) and 99.96 (RFP). Patients with a T cell count below the cut-off value were classified as low, the others as high. A log-rank test was performed to calculate the difference in OS and RFP. Statistical significance of the survival distribution was analyzed by log-rank testing and differences were considered significant when  $p < 0.05$ , as indicated as \* $p < 0.05$ , \*\* $p < 0.01$ , \*\*\* $p < 0.001$  and \*\*\*\* $p < 0.0001$ .



Supplemental figure 4. Continued



**Supplemental figure 5. Clustering analysis using CITRUS revealed 10 distinctive populations of CD4<sup>+</sup> and CD8<sup>+</sup> T cells.** Automatic discovery of stratifying biological signatures to identify significantly different cell populations within tumor and blood samples was performed using the CITRUS algorithm ( $n=52$ , 11 healthy controls, 29 VSCC PBMC and 12 VSCC tumors). Analyses were done within the total CD3<sup>+</sup> immune population for T cells. Phenotypic plots showing expression of the indicated cell surface markers for the identified CD8<sup>+</sup> T cell (# 1 to 5) and CD4<sup>+</sup> T cell (#6 to 10) populations. Expression of the designated markers is given in purple for the total analysed immune cells and in red for the clustered cells (overlay).



**Supplemental figure 6. Gating strategy for CD8<sup>+</sup>, non-Treg CD4<sup>+</sup> and regulatory (Treg) T cell populations.** Characterization was done according to our previously publications on Treg and Tbet gating.<sup>31</sup> Gating strategy is depicted for a representative VSCC tumor sample. (A) Following doublet and dead cell exclusion, CD3<sup>+</sup> T cells were selected, which were further divided on the basis of CD4 and CD8 expression. Total CD8<sup>+</sup> T cells are gated in green. Within the CD4<sup>+</sup> T cells, CD25<sup>+</sup>CD127<sup>-</sup> cells (red) were selected for further Foxp3 gating (Foxp3<sup>+</sup> Tregs) and the non CD25<sup>+</sup>CD127<sup>-</sup> CD4<sup>+</sup> T cells for further non-Treg CD4 gating (in blue). (B) Expression of the transcription factor Tbet (top panel), and the checkpoint molecules Tim-3 (middle panel) and Lag-3 (bottom panel) within CD3<sup>+</sup>CD8<sup>+</sup> T cells (left), non-Treg CD3<sup>+</sup>CD4<sup>+</sup> T cells (middle) and CD4<sup>+</sup>CD25<sup>+</sup>CD127<sup>-</sup>Foxp3<sup>+</sup> T cells (right).

Supplemental table 1. Antibody panels.

	Antibody	Antigen	Detection	Fluorochrome	Clone	Supplier
Multiplex immunofluorescent staining	panel 1					
	1	Pan-cytokeratin	Direct	Alexa647	AE1/AE3, C11	Thermo fisher scientific
	2	PD1	Indirect	OPAL520	D4W2J	Cell signaling Technology
	3	CD8	Indirect	CF555	4B11	DAKO
	4	Foxp3	Indirect	CF633	236A/E7	eBioscience
	5	CD3	Direct	Alexa594	D7A6E	Cell signaling Technology
		DAPI				
	panel 2					
	1	Pan-cytokeratin	Direct	Alexa647	AE1/AE3, C11	Thermo fisher scientific
	2	Tbet	Indirect	OPAL520	H-210	Santa Cruz
3	CD3	Direct	Alexa594	D7A6E	Cell signaling Technology	
	DAPI					
Flowcytometry antibody panel	1	CD45		PerCP-Cy5.5	2D1	BD Biosciences
	2	CD3		V450	UCHT1	BD Biosciences
	3	CD4		AlexaFluor700	RPA-T4	BD Biosciences
	4	CD8		PE-CF594	RPA-T8	BD Biosciences
	5	CD103		BV605	Ber-ACT8	Biolegend
	6	CD161		PE	HP-3G10	Biolegend
	7	CD38		BV650	HB-7	Biolegend
	8	HLA-DR		V500	G46-6	BD Biosciences
	9	PD-1		PE-Cy7	EH12.2H7	Biolegend
	10	NKG2a		APC	Z199	Beckman Coulter
	11	CD45RA		APC-H7	HI100	BD Biosciences
	12	CCR7		AlexaFluor488	G043H7	Biolegend
	13	CD3		V500	UCHT1	BD Biosciences
	14	CD8		BB700	HIT8a	BD Biosciences
	15	CD25		PE-Cy7	2A3	BD Biosciences
	16	CD127		BV650	A019D5	Biolegend
	17	TIM-3		BV605	F38-2E2	Biolegend
	18	LAG-3		BV421	11C3C65	Biolegend
	19	KLRG-1		APC	13F12F2	eBiosciences
	20	Foxp3		PE-CF594	259D/C7	BD Biosciences
	21	Ki67		FITC	20Raj1	eBiosciences
	22	Tbet		PE	ebio4B10	eBiosciences

Supplemental table 2. Patient characteristics of 65 primary VSCC samples.

Characteristic (n, %)	HPVpos (n=23)	HPVneg/p53wt (n=20)	HPVneg/p53mut (n=22)	p-value
Age – yr (median, range)	60 (40-89)	70.5 (47-91)	77.5 (41-86)	<b>0.013</b>
<b>Smoking</b>				<b>0.005</b>
No	5 (21.7%)	12 (60%)	14 (63.6%)	
Current	15 (65.2%)	3 (15%)	3 (13.6%)	
Non-current	1 (4.3%)	2 (10%)	1 (4.5%)	
Unknown	2 (8.7%)	3 (15%)	4 (18.2%)	
<b>Immunosuppression</b>				-
HIV	-	-	-	
Immunosuppressive	2 (8.7%)	-	-	
<b>FIGO stadium</b>				0.429
IA	2 (8.7%)	1 (5%)	-	
IB	21 (91.3%)	19 (95%)	21 (95.5%)	
II	-	-	-	
IIIA	-	-	1 (4.5%)	
<b>Size tumor in cm</b>				0.450
≤2cm	15 (65.2%)	9 (45%)	10 (45.5%)	
2-4cm	5 (21.7%)	7 (35%)	6 (27.3%)	
≥4cm	2 (8.7%)	4 (20%)	6 (27.3%)	
<b>Depth of invasion in mm</b>				0.129
≤4mm	15 (65.2%)	7 (35%)	11 (50%)	
>4mm	7 (30.4%)	12 (60%)	11 (50%)	
<b>LVSI</b>				0.414
No	20 (87%)	19 (95%)	18 (81.8%)	
Yes	1 (4.3%)	-	3 (13.6%)	
Unknown	2 (8.7%)	1 (5%)	1 (4.5%)	
<b>Perineural growth</b>				0.245
No	10 (43.5%)	12 (60%)	9 (40.9%)	
Yes	-	-	2 (9.1%)	
Unknown	13 (56.5%)	8 (40%)	11 (50%)	
<b>Positive margin</b>				0.371
No	23 (100%)	20 (100%)	21 (95.5)	
Yes	-	-	1 (4.5%)	
<b>HPV genotyping</b>				-
Type 16	19 (82.6%)	-	-	
Type 18	1 (4.3%)	-	-	
Type 33	2 (8.6%)	-	-	
Type 53	1 (4.3%)	-	-	
<b>Treatment modality</b>				0.646
Surgery	22 (95.7%)	19 (95%)	21 (95.5%)	
Surgery & (chemo)radiotherapy	1 (4.3%)	1 (5%)	1 (4.5%)	
<b>Recurrence</b>				<b>0.006</b>
No	20 (87%)	12 (60%)	9 (40.9%)	
Yes	3 (13%)	8 (40%)	13 (59.1%)	
Local (first recurrence)	3 (100%)	6 (75%)	12 (92.3%)	
Locoregional (first recurrence)	-	2 (25%)	1 (7.7%)	
Distant (first recurrence)	-	-	-	
<b>Time to first recurrence in months (median, range)</b>				0.794
	30 (9-42)	34 (11-103)	32 (7-125)	
<b>Survival status</b>				<b>0.014</b>
Alive	22 (95.7%)	14 (70%)	13 (59.1%)	
Dead	1 (4.3%)	6 (30%)	9 (40.9%)	

Significant *p*-values <0.05 by group comparison analysis of categorical data by chi-square test are shown in bold. For non-parametric continuous variables, the Mann-Whitney U test was used. LVSI = lymphovascular space invasion.

**Supplemental table 3. Statistical differences in T cell infiltration between VSCC subtypes and healthy controls.**

	<b>Controls</b> median (range) <i>n</i> =10	<b>HPVpos</b> median (range) <i>n</i> =23	<b>HPVneg/p53wt</b> median (range) <i>n</i> =20	<b>HPVneg/p53mut</b> median (range) <i>n</i> =22
CD3 <sup>+</sup> total (E)	182.97 (20.76-851.13)	284.6 (17.0-1383.07)	242.62 (13.78-2719.33)	131.83 (12.55-641.09)
CD3 <sup>+</sup> total (S)	241.13 (90.07-872.49)	1307.51 (33.79-8452.21)	749.11 (203.67-4719.74)	618.32 (35.12-2043.65)
CD3 <sup>+</sup> total (T)	456.76 (183.86-1568.55)	1484.48 (115.01-9011.90)	949.54 (238.87-5729.06)	755.90 (49.97-2684.73)
CD3 <sup>+</sup> CD8 <sup>+</sup> Foxp3 <sup>-</sup> (E)	68.06 (13.12-774.77)	124.21 (3.82-606.15)	72.76 (13.78-2325.93)	37.70 (2.26-451.38)
CD3 <sup>+</sup> CD8 <sup>+</sup> Foxp3 <sup>-</sup> (S)	134.97 (28.79-667.79)	517.29 (6.47-5138.58)	401.25 (94.64-1589.67)	295.60 (18.38-1493.11)
CD3 <sup>+</sup> CD8 <sup>+</sup> Foxp3 <sup>-</sup> (T)	190.18 (41.92-1442.56)	705.26 (37.58-5487.34)	469.08 (129.82-3915.60)	332.03 (24.79-1944.50)
CD3 <sup>+</sup> CD8 <sup>+</sup> Foxp3 <sup>+</sup> (E)	66.27 (4.42-185.51)	96.2 (3.57-759.69)	63.76 (0.00-1222.17)	41.30 (0.00-169.71)
CD3 <sup>+</sup> CD8 <sup>+</sup> Foxp3 <sup>+</sup> (S)	86.90 (20.02-331.15)	472.48 (20.17-3150.50)	114.24 (0.00-2506.14)	119.81 (7.07-483.01)
CD3 <sup>+</sup> CD8 <sup>+</sup> Foxp3 <sup>+</sup> (T)	158.18 (88.81-516.66)	612.94 (40.34-3578.03)	226.92 (0.00-3580.08)	249.98 (7.07-581.70)
CD3 <sup>+</sup> CD8 <sup>+</sup> Foxp3 <sup>+</sup> (E)	5.15 (1.72-28.84)	44.05 (0.00-1383.07)	80.13 (0.00-285.71)	26.04 (0.00-268.88)
CD3 <sup>+</sup> CD8 <sup>+</sup> Foxp3 <sup>+</sup> (S)	27.11 (1.85-96.61)	173.04 (0.00-1631.58)	193.24 (0.00-793.29)	152.49 (3.87-458.11)
CD3 <sup>+</sup> CD8 <sup>+</sup> FoxP3 <sup>+</sup> (T)	38.46 (7.96-125.45)	244.68 (0.00-1642.67)	347.76 (0.00-1012.27)	200.43 (6.60-521.08)
CD3 <sup>+</sup> PD1 <sup>+</sup> (E)	41.94 (0.00-200.55)	126.32 (5.13-1034.34)	94.4 (0.00-551.40)	24.07 (0.00-257.71)
CD3 <sup>+</sup> PD1 <sup>+</sup> (S)	125.58 (0.00-1041.00)	281.9 (27.11-3031.92)	177.69 (0.00-1386.38)	62.76 (0.00-451.26)
CD3 <sup>+</sup> PD1 <sup>+</sup> (T)	196.16 (0.00-509.04)	303.85 (32.23-3750.06)	304.3 (0.00-1937.78)	99.98 (0.00-593.37)

*p*-values between two groups were analyzed by non-parametric Mann-Whitney U test to determine differences in T cell subset infiltration between healthy controls, HPVpos VSCC, HPVneg/p53wt VSCC, and HPVneg/p53mut VSCC. Significant differences are indicated in bold. (E)= epithelium, (S) = stroma, (T) = total.

<i>p</i> -value Controls vs HPVpos	<i>p</i> -value Controls vs HPVneg/p53wt	<i>p</i> -value Controls vs HPVneg/p53mut	<i>p</i> -value HPVpos vs HPVneg/p53wt	<i>p</i> -value HPVpos vs HPVneg/p53mut	<i>p</i> -value HPVneg/p53wt vs HPVneg/p53mut
0.144	0.397	0.675	0.697	<b>0.029</b>	0.059
<b>0.002</b>	0.004	<b>0.018</b>	0.368	<b>0.018</b>	0.290
<b>0.003</b>	<b>0.028</b>	0.119	0.374	<b>0.017</b>	0.217
0.269	0.713	0.483	0.609	<b>0.026</b>	0.102
<b>0.005</b>	<b>0.010</b>	0.070	0.436	0.056	0.247
<b>0.010</b>	0.044	0.268	0.336	<b>0.028</b>	0.257
0.305	0.948	0.305	0.318	<b>0.014</b>	0.371
<b>0.009</b>	0.746	0.388	0.058	<b>0.007</b>	0.762
<b>0.008</b>	0.746	0.826	0.056	<b>0.004</b>	0.960
<b>0.006</b>	<b>0.0002</b>	<b>0.012</b>	<b>0.008</b>	0.725	<b>0.026</b>
<b>0.007</b>	<b>0.001</b>	<b>0.001</b>	0.724	0.570	0.208
<b>0.004</b>	<b>0.0001</b>	<b>0.001</b>	0.408	0.467	0.078
<b>0.031</b>	0.231	0.458	0.173	<b>0.0001</b>	<b>0.006</b>
0.089	0.267	0.483	0.527	<b>0.001</b>	<b>0.012</b>
0.006	0.074	0.562	0.422	<b>0.0001</b>	<b>0.012</b>

Supplemental table 4. Pearson correlations between the numbers of intraepithelial and stromal T cells.

		Intraepithelial cell count				
		CD3 <sup>+</sup>	CD3 <sup>+</sup> CD8 <sup>-</sup> Foxp3 <sup>-</sup>	CD3 <sup>+</sup> CD8 <sup>+</sup> Foxp3 <sup>-</sup>	CD3 <sup>+</sup> CD8 <sup>-</sup> Foxp3 <sup>+</sup>	CD3 <sup>+</sup> PD1 <sup>+</sup>
Intraepithelial cell count	CD3 <sup>+</sup>		0.870 <b>p=0.000</b>	0.766 <b>p=0.000</b>	0.551 <b>p=0.000</b>	0.462 <b>p=0.000</b>
	CD3 <sup>+</sup> CD8 <sup>-</sup> Foxp3 <sup>-</sup>			0.373 <b>p=0.002</b>	0.354 <b>p=0.004</b>	0.246 <b>p=0.048</b>
	CD3 <sup>+</sup> CD8 <sup>+</sup> Foxp3 <sup>-</sup>				0.378 <b>p=0.002</b>	0.590 <b>p=0.000</b>
	CD3 <sup>+</sup> CD8 <sup>-</sup> Foxp3 <sup>+</sup>					0.179 p=0.153
	CD3 <sup>+</sup> PD1 <sup>+</sup>					
Invasive border cell count	CD3 <sup>+</sup>	0.956 <b>p=0.000</b>	0.826 <b>p=0.000</b>	0.732 <b>p=0.000</b>	0.550 <b>p=0.000</b>	0.356 <b>p=0.004</b>
	CD3 <sup>+</sup> CD8 <sup>-</sup> Foxp3 <sup>-</sup>	0.858 <b>p=0.000</b>	0.978 <b>p=0.000</b>	0.367 <b>p=0.003</b>	0.383 <b>p=0.002</b>	0.174 p=0.166
	CD3 <sup>+</sup> CD8 <sup>+</sup> Foxp3 <sup>-</sup>	0.742 <b>p=0.000</b>	0.370 <b>p=0.002</b>	0.953 <b>p=0.000</b>	0.379 <b>p=0.002</b>	0.487 <b>p=0.000</b>
	CD3 <sup>+</sup> CD8 <sup>-</sup> Foxp3 <sup>+</sup>	0.593 <b>p=0.000</b>	0.442 <b>p=0.000</b>	0.382 <b>p=0.002</b>	0.886 <b>p=0.000</b>	0.137 p=0.278
	CD3 <sup>+</sup> PD1 <sup>+</sup>					
Stromal cell count	CD3 <sup>+</sup>	0.449 <b>p=0.000</b>	0.344 <b>p=0.005</b>	0.477 <b>p=0.000</b>	0.212 p=0.090	0.415 <b>p=0.001</b>
	CD3 <sup>+</sup> CD8 <sup>-</sup> Foxp3 <sup>-</sup>	0.279 <b>p=0.024</b>	0.346 <b>p=0.005</b>	0.163 <b>p=0.194</b>	0.106 p=0.399	0.338 <b>p=0.006</b>
	CD3 <sup>+</sup> CD8 <sup>+</sup> Foxp3 <sup>-</sup>	0.490 <b>p=0.000</b>	0.226 <b>p=0.001</b>	0.692 <b>p=0.000</b>	0.219 p=0.079	0.348 <b>p=0.004</b>
	CD3 <sup>+</sup> CD8 <sup>-</sup> Foxp3 <sup>+</sup>	0.265 <b>p=0.033</b>	0.101 p=0.423	0.316 <b>p=0.010</b>	0.279 <b>p=0.025</b>	0.228 p=0.068
	CD3 <sup>+</sup> PD1 <sup>+</sup>	0.221 p=0.076	0.333 p=0.797	0.389 <b>p=0.001</b>	0.120 p=0.341	0.594 <b>p=0.000</b>

Significant *p*-values <0.05 are shown in bold.

Supplemental table 5. Median and optimized cut-off point by ROC curve analysis per phenotype and outcome.

Intraepithelial phenotype	Recurrence-free period					
	ROC cut-off (cells/mm <sup>2</sup> )	HR-ratio (95% CI)	p-value	Median (cells/mm <sup>2</sup> )	HR-ratio (95%CI)	p-value
CD3 <sup>+</sup>	192.70	4.16 (1.59-10.89)	<b>0.004</b>	637.84	2.89 (1.17-7.16)	<b>0.022</b>
CD3 <sup>+</sup> CD8 <sup>+</sup> Foxp3 <sup>-</sup>	61.82	4.85 (1.87-12.59)	<b>0.001</b>	179.1	2.84 (1.15-7.01)	<b>0.024</b>
CD3 <sup>+</sup> CD8 <sup>+</sup> Foxp3 <sup>+</sup>	37.96	1.76 (0.71-4.40)	0.224	115.71	1.20 (0.50-2.90)	0.604
CD3 <sup>+</sup> CD8 <sup>+</sup> Foxp3 <sup>+</sup>	38.71	1.42 (0.59-3.44)	0.439	77.78	1.42 (0.59-3.44)	0.439
CD3 <sup>+</sup> PD1 <sup>+</sup>	99.96	2.66 (1.09-6.51)	<b>0.032</b>	130.04	2.27 (0.94-5.52)	0.070
Overall survival						
CD3 <sup>+</sup>	309.40	4.97 (1.38-17.88)	<b>0.014</b>	637.84	8.23 (2.37-28.51)	<b>0.009</b>
CD3 <sup>+</sup> CD8 <sup>+</sup> Foxp3 <sup>-</sup>	82.58	6.24 (1.79-21.76)	<b>0.004</b>	179.10	5.30 (1.53-18.36)	<b>0.009</b>
CD3 <sup>+</sup> CD8 <sup>+</sup> Foxp3 <sup>-</sup>	35.63	3.00 (0.81-0.09)	0.097	115.71	3.21 (0.93-11.09)	0.065
CD3 <sup>+</sup> CD8 <sup>+</sup> Foxp3 <sup>+</sup>	54.58	3.01 (0.87-1.42)	0.083	77.78	2.48 (0.716-8.59)	0.152
CD3 <sup>+</sup> PD1 <sup>+</sup>	37.67	2.95 (0.74-11.69)	0.125	130.04	2.62 (0.75-9.14)	0.132

Significant p-values <0.05 are shown in bold.

Supplemental table 6. Uni- and multivariate analysis for recurrence-free period and overall survival.

Variable	Recurrence-free period total cohort				Recurrence-free period HPVneg VSCC only			
	HR crude	p-value	HR adjusted	p-value	HR crude	p-value	HR adjusted	p-value
Intraepithelial CD3 <sup>+</sup> CD8 <sup>+</sup> FoxP3 <sup>-</sup> (low/high)	4.11 (1.62-10.39)	<b>0.003</b>	3.31 (1.22-8.94)	<b>0.018</b>	3.14 (1.15-8.57)	<b>0.026</b>	3.07 (1.07-8.83)	<b>0.038</b>
Age	1.04 (1.00-1.07)	<b>0.037</b>	1.02 (0.98-1.06)	0.281	1.02 (0.98-1.06)	0.321	1.01 (0.97-1.05)	0.586
P53-IHC (wildtype/mutant)	0.62 (0.26-1.49)	0.283	1.33 (0.47-3.72)	0.591	0.85 (0.32-2.23)	0.734	1.21 (0.43-3.43)	0.721
HPV (negative/positive)	2.47 (0.72-8.44)	0.149	1.99 (0.51-7.74)	0.320				
Intraepithelial CD3 <sup>+</sup> (low/high)	3.49 (1.41-8.61)	<b>0.007</b>	2.95 (1.05-8.25)	<b>0.040</b>	3.33 (1.22-9.08)	<b>0.019</b>	3.66 (1.19-11.26)	<b>0.024</b>
Age	1.04 (1.00-1.07)	<b>0.037</b>	1.02 (0.98-1.06)	0.288	1.02 (0.98-1.06)	0.321	1.01 (0.97-1.05)	0.688
P53-IHC (wildtype/mutant)	0.62 (0.26-1.49)	0.283	1.53 (0.53-4.43)	0.438	0.85 (0.32-2.23)	0.734	1.50 (0.50-4.45)	0.470
HPV (negative/positive)	2.47 (0.72-8.44)	0.149	2.18 (0.56-8.49)	0.261				

Significant p-values <0.05 are shown in bold.

